Universitat Autònoma de Barcelona

Design of Network Coding Functionality for 5G Networks

Tan Do-Duy

Design of Network Coding Functionality for 5G Networks

Tan Do-Duy

Supervisor: Prof. M. Ángeles Vázquez-Castro

Ph.D. Programme in Electrical Engineering and Telecommunications
Department of Telecommunications and Systems Engineering
Autonomous University of Barcelona

This thesis is submitted for the degree of
Ph.D. in Telecommunications and Systems Engineering

School of Engineering September 2018

PH.D. THESIS: DESIGN OF NETWORK CODING FUNCTIONALITY FOR 5G NETWORKS

PH.D. CANDIDATE: TAN DO-DUY

SUPERVISOR: PROF. MARIA ÁNGELES VÁZQUEZ-CASTRO

PH.D. PROGRAMME IN ELECTRICAL ENGINEERING AND TELECOMMUNICATIONS
Department of Telecommunications and Systems Engineering
School of Engineering
Autonomous University of Barcelona
Bellaterra, September 10th, 2018

Acknowledgements

First of all, I would like to express my deep gratitude and appreciation to my thesis supervisor, Professor Maria Ángeles Vázquez-Castro, for her invaluable support, expert guidance and comments during my PhD study. Her patience and enthusiasm has encouraged me a lot to overcome the most difficult time and complete this final phase.

Throughout the PhD course, fortunately I had an opportunity to co-work with AnsuR Technologies and Simula Research Laboratory in Oslo, Norway, for the EU GEO-VISION project and part of the EU HENCSAT project, which inspired the study cases in this thesis. I would like to thank Dr. Harald Skinnemoen, Dr. Ozgu Alay, and Dr. Thomas Dreibholz for their collaborative work, support, and guidance to address practical issues in communication networks.

I would like to thank my lab-mates at UAB, Paresh, Nacho, Helem, and Hina for having helpful discussions both technical and non-technical problems. I would also like to thank all of my friends in Barcelona, Dung, Zacharias, Oanh, Viet, Hoan, Nhung, Vinh, we shared difficulties when living away from home country.

Most importantly, I would like to express my heartfelt gratitude to my grandparents, my parents, my aunts, and my younger sister for their unconditional love and care and especially to my fiancée Cuc who has understood and encouraged me every day to finish this work. Without their encouragement and patience throughout my academic career, none of my achievements would have been possible. This thesis is dedicated to my big family.

Abstract

Network coding (NC) has recently emerged as a new solution for improving network performance in terms of throughput and reliability. Coding operations over the network information flows can be performed both at the source and at intermediate nodes where re-encoding operations allow capacity achievability both for noiseless and noisy networks. However, the multi-user nature of NC and its inherent applicability to versatile flow engineering across all layers of the protocol stack, call for novel wireless system design approaches. The goal of this thesis is to study the design of NC as a network functionality offered to the 5G wireless communication service designers. The design would facilitate the control of network throughput, reliability, and connectivity over 5G wireless networks. The main objectives of this thesis are: (i) to develop a packet-level NC architectural design that could work as a traditional network function (NF) or be easily integrated in current proposals of virtualized network architectures, (ii) to develop a matricial model that allows us to analyze the corresponding error probabilities of different NC schemes over multi-hop line networks, a simple but common in practice network model, (iii) to develop a methodology to compute and evaluate the finite-length coding performance of different NC schemes which could be selected as the operational NC scheme for the designed NC functionality (NCF), and (iv) to apply the proposed NCF design and validate its performance for a complete use case in 5G networks.

The contributions of this thesis are the following. We first develop a design of Network Coding Functionality as a toolbox of NC design domains and show how it can be integrated in current virtualized infrastructures. Second, we evaluate the finite-length performance of different network codes using random vs Pascal matrices. We model the encoding, re-encoding, and decoding process of different coding schemes in matrix notation and corresponding error probabilities. We then propose a binary searching algorithm to identify optimal coding rate for some specific target packet loss rates given a pre-defined coding block-length. We will focus on capacity-achieving codes and coding schemes with scheduling for representative scenarios and show the achievable rate-delay trade-off between random codes and structured codes with scheduling. In the last part of this thesis, we validate the proposed NCF design for a complete use case to enhance connectivity of Mobile Ad-hoc Network

(MANET) devices over converged satellite-cloud networks in emergency applications. The key insight is that in an emergency scenario there may not be direct access to fog or cloud computing, which will then be provided via satellite and the only local computational resources available are the MANET devices. To solve this situation, we define a packet-level NCF with inputs from data service quality targets, local computation constraints and per-path statistics. Outputs are centrally-optimized coding rates balancing per-node computational resources and resulting coverage.

Table of contents

List of figures

List of tables

Abbreviations

Table 1 List of Abbreviations

5G	Fifth generation mobile networks
D2D	Device-to-Device
ETSI	The European Telecommunications Standards Institute
GEO-VISION	GNSS driven EO and Verifiable Image and Sensor Integration for mission-critical Operational Networks
HENCSAT	Network Coding Protocols for Satellite Terminals with Multiple Logical Paths
IRTF	Internet Research Task Force
MANET	Mobile Ad-hoc Network
MANO	Management and Orchestration
NC	Network Coding
NCF	Network Coding Functionality
NF	Network Function
NFV	Network Function Virtualization
NFVI	NFV Infrastructure
PascalNC	SNC using Pascal coefficients
PascalNC-S	PascalNC with Scheduling
PLR	Packet Loss Rate
RLNC	Random Linear Network Coding
SDN	Software-Defined Networking
SNC	Systematic Network Coding
SNC-S	SNC with packet Scheduling
SWNC	Sliding Window Network Coding
VIM	Virtualized Infrastructure Manager
VNF	Virtualized Network Function
VNFM	VNF Manager
VM	Virtual Machine

Chapter 1

Introduction

1.1 Motivation

NC has attracted much attention in recent years as key concepts for 5G networks to provide flexibility and substantial gains in network throughput and reliability [2–7]. The performance of NC depends on the deployment of special nodes on the path, known as the coding points, that perform re-encoding the coded packets from the source in order to allow capacity achievability both for noiseless [8] and noisy networks [9].

From a practical point of view, the multi-user nature of NC and its inherent applicability to versatile flow engineering across all layers of the protocol stack, call for novel wireless system design approaches. As a result, there is a need for a possible way forward to the design of NC as a network functionality offered to the 5G wireless communication service designers. There are already prototypes that show the integration of NC into current proposals of virtualized architectures. For example, authors in [3, 6] provided a prototype with the implementation of NC as an additional NF via virtual machines (VMs) by sharing system resources. More recently, an adaptive NC scheme is proposed in [4] to enhance the transmission efficiency for the Internet of things core network with Software-Defined Networking (SDN) formed by the smart devices. The coding rate of NC can be adjusted in a centralized manner at the SDN controller. However, a unified framework for the design of NC as a NF is currently missing.

Therefore, the goal of this thesis is to design and evaluate the performance of a packet-level Network Coding Functionality, NCF, operating as a NF to facilitate the control of network throughput and reliability over 5G wireless networks. We then work out a complete case study for controlled achievable rate and connectivity of MANET devices over converged satellite-cloud networks in emergency applications where providing reliable communication services over wireless networks is a challenging problem due to high packet loss rates and stringent delivery requirements of the emergency services. The communication scenario in

this thesis is part of the network model in the EU H2020 GEO-VISION research project [10], where the application was packet-level NC to provide reliable video transmission in situational awareness scenarios. More specifically, our work proposes a NCF design that could work as a traditional NF or be integrated with virtualization technology so that tailored designs can be implemented in software and deployed over virtualized infrastructures e.g., Network Function Virtualization (NFV) [1] and/or SDN [11, 12]. We then measure and analyze the performance of the proposed NCF in terms of achievable rate and connectivity for some data service quality targets, local computation resources at the nodes, and per-path link statistics.

1.2 Objectives

Based on the motivation described above, the high-level objectives of this thesis are the following:

- **Objective 1: Develop a packet-level NC architectural design that could work as a traditional NF or be easily integrated in current proposals of virtualized network architectures.**
  - Our first objective focuses on developing a NC architectural design with a generic functional design. The proposed design will be then integrated into the current virtualized network architectures e.g., NFV and SDN, as a toolbox of NC design domains so that NC can be implemented as a NF (i.e., NCF) over different physical networks.
- **Objective 2: Develop a matricial model that allows us to analyze the corresponding error probabilities of different NC schemes over multi-hop line networks, a simple but common in practice network model.**
  - As part of the NC coding domain in the NC architectural design, we first develop a generic matricial model that will allow us to model the encoding, re-encoding and decoding function of different NC schemes. We then provide an in-depth analysis of the corresponding packet loss rates (PLRs) of the considered NC schemes over multi-hop line networks. This should be obtained via theoretical analysis and/or simulation results.
- **Objective 3: Develop a methodology to compute and evaluate the finite-length performance of different NC schemes which could be selected as the operational NC scheme for the designed NCF.**

  - Our next objective is to propose a methodology to compute the optimal finite-length coding rate and achievable rate for different NC schemes over line networks given a pre-defined coding block-length for some target PLR requirements. The results obtained by applying the proposed methodology for representative network scenarios will reveal the pros and cons in terms of achievable rate and average in-order packet delay at the destination node, and coding overhead with regard to different NC schemes. This is useful for the selection of the operational NC scheme for the NCF proposed in the first objective.

- **Objective 4: Apply the NCF design developed in Objective 1 and validate its performance for a complete use case in 5G network scenarios.**

  - Our forth objective is to apply and validate the NCF design achieved from the above objectives for a study case e.g., enhancing connectivity of MANET devices over converged satellite-cloud networks in an emergency situation where the communication scenario is part of the network model in the EU H2020 GEO-VISION project [10]. Specifically, we propose the use of per-flow NC which is provided by a NCF. The inputs of the NCF are from data service quality targets, computational resources, and per-path statistics whereas the outputs are the optimal finite-length coding rates balancing per-node computational resources and resulting coverage.

This thesis has taken and generalized the ideas developed and solved in the EU H2020 GEO-VISION project to an academic level with the appropriate modeling.

1.3 Structure and Contributions of the Dissertation

We have studied the design of a Network Coding Functionality by first proposing the design domains of NC and the integration of NC as a NF into current virtualized architectures, then modeling and evaluating the performance of different NC schemes which could be used by the NCF. Finally, we validate the proposed NCF design for a complete use case to enhance the reliability of communication over converged satellite-cloud networks in an emergency situation.

The structure of this thesis is based on the main objectives reflected in Chapters 3-6. More specifically, the contributions per chapter are summarized as follows:

- **Chapter 1 introduces the doctoral thesis.** This chapter presents the motivation, objectives and major contributions of the thesis. Furthermore, we introduce the structure of this thesis and the list of the contributions related to the work in the thesis.

- **Chapter 2 provides the reader with the preliminaries on the context used in this thesis.** In particular, we first describe the preliminaries on the network scenario that we will use for the use case to validate the performance of the proposed NCF. Second, we justify our proposed work with respect to the state-of-the-art. Then, we review some applications of NC for emergency situations. Finally, considering video or images as illustrative traffic for the use case, we provide a literature review of NC applications for delay-constrained network services over multi-hop wireless networks.

- **Chapter 3 focuses on the design of Network Coding Functionality as a toolbox of NC design domains.** This chapter contributes to the achievement of Objective 1. The main contributions from this chapter are as follows.

  - We propose an architectural design for NC which includes a functional domain design that enables virtualization-based design.
  - We also illustrate the integration of the proposed NC design into virtualized infrastructures e.g., SDN and NFV, as a toolbox of NC design domains to allow flow engineering tailored to service operational intent.

- **Chapter 4 focuses on evaluating the finite-length performance of different network codes which could be selected as the operational network code for the NCF.** This chapter contributes to the achievement of Objectives 2 and 3 by modeling and comparing the performance of different linear NC schemes (using random and Pascal (algebraic) coefficients) over multi-hop line networks. The main contributions from this chapter are as follows.

  - We model the encoding, re-encoding, and decoding process of different linear coding schemes in matrix notation and corresponding error probabilities.
  - We propose a binary searching algorithm to identify optimal coding rate for some specific target PLRs given a pre-defined coding block-length.
  - We apply the proposed methodology to compute the optimal finite-length coding rate, achievable rate, and average in-order packet delay for representative number of links and per-link erasure rates. Our simulation results show that for small block-length, the optimal coding rates follow exponential behaviour which could be a challenging issue for the designer of adaptive NC solutions. Further, our methodology is useful to characterize the throughput/delay trade-off between capacity-achieving vs non-capacity achieving schemes in the finite-length regime. Our results aim to guide the network designer to identify the best choice of practical codes and coding rates depending on the user-case.

- **Chapter 5 focuses on the validation of the proposed NCF design for a complete use case to enhance the connectivity of MANET devices over converged satellite-cloud networks in emergency applications.** This chapter contributes to the achievement of Objective 4 by presenting a complete solution to tackle the problem of enhancing MANETs coverage for emergency scenarios. The main contributions from this chapter are as follows.
  - We define a packet-level NCF with inputs from data service quality targets, local computation constraints and per-path statistics. Outputs are optimal coding rates balancing per-node computational resources and resulting coverage.
  - We formulate, solve and analyze the centrally-controlled optimization problem for typical values of computational resources at the nodes.
  - Simulation results show that our solution not only makes connectivity possible, but also provides gains of orders of magnitude with respect to currently used routing.
- **Finally, Chapter 6 draws the final conclusions of the thesis and proposes the future lines of research.**

1.4 List of Contributions

The work leading to this thesis has been presented in different scientific publications as well as in a number of project deliverable reports. Following are the list of contributions:

JOURNALS

1. **Tan Do-Duy**, P. Saxena, and M. A. Vázquez-Castro, "Finite-length Performance Comparison of Network Codes using Random vs Pascal Matrices", *under review in IEEE Wireless Communications Letters (Q1, IF=3.096)*, August 2018.
2. **Tan Do-Duy** and M. A. Vázquez-Castro, "Network Coding Function for Converged Satellite-Cloud Networks", *under review in IEEE Transactions on Aerospace and Electronic Systems (Q1, IF=2.063)*, August 2018.
3. **Tan Do-Duy** and M. A. Vázquez-Castro, "Finite-length Network Coding for Integrated MANETs-Satellite Networks", *under review in Elsevier Ad Hoc Networks (Q1, IF=3.151)*, September 2018.

CONFERENCES

1. **Tan Do-Duy** and M. A. Vázquez-Castro, "Geo-Network Coding Function Virtualization for Reliable Communication over Satellite", in *Proc. IEEE International Conference on Communications (ICC)*, Paris, France, May 2017 **(one of the two flagship conferences of the IEEE Communications Society)**.

2. **Tan Do-Duy** and M. A. Vázquez-Castro, "Network Coding Function Virtualization", in *Proc. The 17th IEEE International Workshop on Signal Processing Advances in Wireless Communications (SPAWC)*, Edinburgh, UK, July 2016 **(the flagship workshop of the Signal Processing for Wireless Communications and Networking Technical Committee of the IEEE Signal Processing Society)**.

3. M. A. Vázquez-Castro, P. Saxena, **Tan Do-Duy**, T. Vamstad, and H. Skinnemoen, "SatNetCode: Functional design and experimental validation of network coding over satellite", in *the International Symposium on Networks, Computers and Communications (ISNCC)*, Rome, Italy, June 2018.

4. **Tan Do-Duy** and M. A. Vázquez-Castro, "Efficient Communication over Cellular Networks with Network Coding in Emergency Scenarios", in *2015 2nd International Conference on Information and Communication Technologies for Disaster Management (ICT-DM)*, Rennes, France, 2015, pp. 71–78.

Contributions to Project Deliverable Reports: EU H2020 GEO-VISION Project (2015-2017)

1. D2: 2.2 Technical Requirements and 2.3 System Design.

2. D3: 3.1 Research Technology, 3.2 Technology Development, and 3.3 Technology Integration Report.

Contributions to the IRTF

1. M.A. Vázquez-Castro, **Tan Do-Duy**, Simon Romano, Antonia Maria Tulino, "Network Coding Function Virtualization", *IETF Internet-Draft*, May 2017.

Chapter 2

Preliminaries

This chapter presents the preliminaries related to our use case of the proposed NCF for enhancing the connectivity of MANET devices over converged satellite-cloud networks in emergency applications. Specifically, Section 2.1 introduces the network scenario for the use case. Section 2.2 justifies our proposed work w.r.t. the-state-of-the-art. Section 2.3 provides an overview of NC for emergency applications. Finally, Section 2.4 introduces some applications of NC for reliable delay-constrained services over multi-hop wireless networks.

2.1 Preliminaries on the network scenario

The system architecture for our use case of the NCF in emergency applications is illustrated in Fig. 2.1. Several communication devices of every MANET have their communication paths defined according to known protocols [13–16] or 5G Device-to-Device (D2D) technology [17–21]. The mobile devices represent e.g. relief teams or any other kind of communication scenario in such an emergency situation. Under such scenario we assume D2D technology to enhance MANETs communication for emergency applications. We assume D2D as it is a promising 5G technology for direct communication between mobile devices [18, 19]. Due to unreliable MANET links, transmission may be highly impaired and coverage reduced, which is very undesirable in an emergency situation. This problem was addressed in the EU H2020 GEO-VISION research project [10], a project for mission-critical communications.

Increasing the MANET connectivity in number of hops to enhance the MANET coverage (to e.g. relief teams) calls for the use of per-flow NC. The use of NC technology [22–24] allows to guarantee reliable transmission over several hops thus ensuring sufficient coverage and reliable exchange of data between devices in the field and headquarters or cloud resources. While it is well known that NC can theoretically achieve capacity, it is also known that computational resources are necessary for the required encoding, re-encoding

and decoding functionalities, which may require high energy consumption of MANET power-limited devices. The usual solution to such computational problem is to access local computational resources such as fog computing resources known as cloudlets or any sort of micro data center that is geographically accessible and suitable for mobile computation.

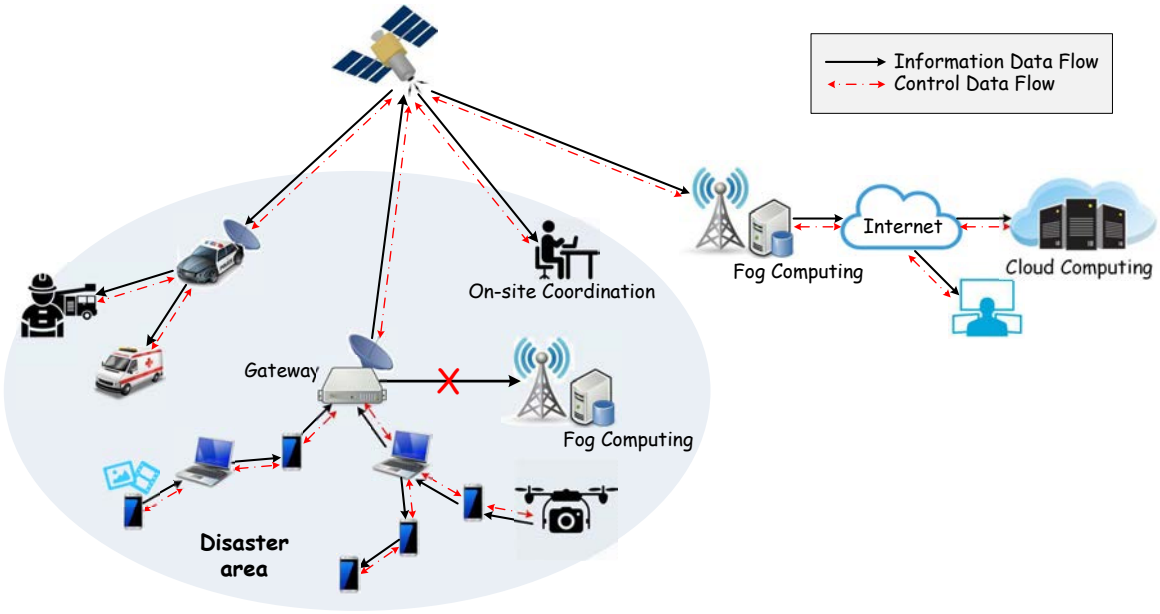

Fig. 2.1 Illustration of a network scenario with MANETs assisted by 5G converged satellite-cloud networks. An emergency situation disconnects MANETs from local terrestrial connectivity and computational resources. Black arrows represent information data flows and red arrows represent control data flow to assist MANET communication.

Within this context, our scenario of interest is the case where there is no access to terrestrial connectivity nor to some local data center for fog computing due to some emergency situation. Hence, the computational issue needs to be addressed in a centralized way, for which we propose the design of a network coding functionality, NCF. This NCF should take as inputs the data service operation quality targets, the local computation constraints and per-link per-path erasure statistics, all available under 5G D2D assumption. The NCF outputs optimal coding rates balancing computational resources and resulting coverage taking into account delay constraints.

2.2 Justification of Our Proposed Scenario w.r.t. the-state-of-the-art

Our proposal differs from state of the art proposals as follows. There are related work considering satellite and/or cloud networks for emergency scenarios [13, 25, 26, 16], however, they differ from our work. For instance, in [13] an architecture was proposed that an emergency network includes temporary mobile stations to allow the communication between the control centers and the first responders in the disaster area through satellite. In another work [25], emergency communication between the first responders and the control centers was performed through either backbone networks or satellite. Yet, in [13, 25] the advantages of the cloud to the management and control of the networks have not been taken into account. More recently, a comparative survey of legacy and emerging technologies for the public safety networks based on Long Term Evaluation was presented in [26]. Furthermore, authors in [16] studied high-level vision of emergency communications in 5G cloud computing paradigm and the challenges that service operators need to overcome in order to satisfy the strict requirements imposed by emergency services. However, the proposed work in [26, 16] does not involve satellite.

In addition, the combination of 5G D2D and the cloud for other scenarios has been studied in various work [17, 27, 28]. For instance, authors in [27] presented a mechanism to reduce energy consumption for data centers in cloud-assisted D2D networks. More recently, in [28] a dynamic algorithm is proposed to reduce energy consumption of both routing and searching services for MANETs assisted by the cloud when link breakages happen due to the mobility of nodes. In [17], authors introduced a D2D based mobile cloud architecture to maintain the communication between devices in public safety applications where a dense deployment of devices is assumed to create a large number of interconnected small mobile clouds with the support of local cloud heads and a SDN controller. However, different from the existing work, we consider the interconnectivity of separate MANETs with the support of the combined satellite-cloud networks.

2.3 Network Coding for Emergency Applications

NC can be classified as either inter-session or intra-session [29]. The former focuses on solving bottleneck problems and reducing the number of transmissions by allowing packets from different sources/flows to be coded together. Therefore, it decreases interference between the links in wireless networks and increases the overall network throughput. However, its drawback is not resilient to packet losses in the system. On the other hand, intra-session NC

leads reliability enhancement in wireless networks with smaller number of transmissions than the feedback-based scheme without NC. This approach exploits the link diversity by combining different packets from the same source/flow. Intra-session NC usually relies on linear network codes to encode and decode packets in a group with coefficients chosen from a finite field.

Emergency communications should be reliable and flexible for disaster aid and relief operation. NC is thus a promising solution to enhance reliability and robustness for data transmission in such scenarios. For example, authors in [30] presented an implementation of network infrastructure with NC to deliver large files from a source to a destination e.g., a real-time video from a cellphone to a helicopter. Intra-session NC is applied at the source node while surrounding nodes simply forward overhearing packets. At the destination, decoding process is performed to recover the original file. NC helps to improve the numbers of files delivered compared to fragmentation in the presence of packet loss or disruptions. The advantages come from spatial diversity by surrounding nodes where various nodes may repeat different pieces of a file due to link disruption by channel condition or busy relays. In [31], NC is employed to improve the packet delivery probability in an intermittently connected network which utilizes mobile networks with cooperation between nodes to create message replication. Main targets are to maximize the delivery ratio and minimize the overhead ratio. In addition, authors in [32] designed a novel NC aided Multi-Input Multi-Output scheme for combating the deleterious effects of both shadow fading and Rayleigh fading in hostile wireless channels. The proposed model leads to ambulance-and-emergency communications. A powerful space-time code is proposed for providing a near-capacity performance in fast fading environments. NC is herein used to obtain a further spatial diversity gain for combating slow fading effects by obstacles. In [33], a novel perceptual semantics for multimedia communications is proposed to enhance situation awareness in human-analysis-driven processes as in emergency operations. The work in [33] mainly focuses on application-layer optimization with adaptive NC at the network layer, which assumes a network architecture as a first-in first-out with finite queue.

2.4 Reliable Delay-constrained Services with NC

Delay-constrained network services e.g., video streaming, are a clear application over MANETs to benefit from the improvements of network throughput and reliability offered by NC [34]. For instance, [35] took into account the importance of video packets in code selection by combining ideas from throughput enhancement and prioritized transmission for improving video quality such as distortion and packet delay. In [36], a joint optimization of

video coding and rate allocation was proposed for video delivery in heterogeneous networks with NC employed at access points in order to minimize the load on the BS. In [37], random linear NC (RLNC) was used at intermediate helpers to minimize the load on the central video servers. However, the paper [37] only considered a two-hop network model between the video servers and end-users connected over the helpers. Most recently, [38] combined layered approach with RLNC into the design of optimal feedback-free broadcast schemes over single-hop networks. Different from the existing work, our work investigates NC as a NF for video streaming over wireless systems with multi-hop coverage extensions. Our main objective is that the transmission of delay-constrained network traffic should be optimized in terms of the efficient use of network resources while meeting the timely delivery requirements of the network services through network-controlled degrees of reliability.

Chapter 3

Network Coding Functionality

Virtualization technologies (e.g. NFV and SDN) have been proposed as a promising design paradigm by the telecommunications sector to facilitate the design, deployment, and management of networking services. Essentially, it separates software from physical hardware so that a network service can be implemented as a set of virtualized network functions (VNFs) through virtualization techniques and run on commodity standard hardware. Therefore, (virtualized) NFs can be instantiated on demand at different network locations without requiring the installation of new equipment. This key idea helps network operators deploy new network services faster over the same physical hardware which reduces capital investment and the time to market of a new service. Now it is the turn for the telecommunications technologies to detach the software from the hardware where the telecommunications functions run. Such detachment demands functionalities and infrastructures to be designed under such new paradigm.

As an innovative technique towards the implementation of NFs, virtualization technologies are clearly a NC design option as it would make NC available as a flow engineering functionality offered to the network. The integration of NC in existing virtualized network architectures will enable the applicability of NC in future networks (e.g., upcoming 5G networks) to both distributed (i.e., each network device) and centralized manners (i.e., servers or service providers). For instance, the European Telecommunications Standards Institute (ETSI) has proposed some use cases for NFV in [39], including the virtualization of cellular base station, mobile core network, home network, and fixed access network, etc.

In this chapter, we first propose an architectural design framework for NC which includes a generic functional design that enables virtualization-based design. We then show how our proposed NC design can be integrated as a NF i.e., a network coding functionality (NCF), in existing virtualized network architectures.

3.1 Contributions and Structure

3.1.1 Contributions of the Chapter

This chapter presents the contributions that meet Objective 1 of this thesis, as defined in Section 1.2:

- **Objective 1: Develop a packet-level NC architectural design that could work as a traditional NF or be easily integrated in current proposals of virtualized network architectures.**
  - Towards the first objective, we propose an architectural design for NC which includes a generic functional design domain that enables virtualization-based design. We also show how NC can be integrated in virtualized infrastructures e.g., NFV and SDN, as a toolbox of NC design domains to allow flow engineering tailored to service operational intent.

3.1.2 Structure of the Chapter

In the rest of this chapter, we first propose NC architectural design domains. In Section 3.3, we define common elementary functionalities of the NC functional design domain. In Section 3.4, we present the integration of NC in current virtualized infrastructures as a NF. Finally, in Section 3.5, we conclude the chapter.

3.2 NC Architectural Design Domains

Follow the design proposal in [40], this section distinguishes three domains for the design of NC engineering solutions.

- **NC coding domain** - domain for the design of network codebooks, encoding/decoding algorithms, performance benchmarks, appropriate mathematical-to-logic maps, etc. Note that this is a domain fundamentally related to coding theory.
- **NC functional domain** - domain for the design of the functional properties of NC to match design requirements built upon abstractions of
  - **Network:** by choosing a reference layer in the standardized protocol stacks and logical nodes for NC and re-encoding operations.

– **System:** by abstracting the underlying physical or functional system at the selected layer e.g. SDN and/or function virtualization.

Note that this is a domain fundamentally related to electrical engineering and computer science. However, note that while traditionally electrical engineering has been concerned with physical networks and computer science with logical networks, virtualization brings both disciplines closer to each other.

- **NC protocol domain** - domain for the design of physical signaling/transporting of the information flow across the virtualized physical networks in one way or interactive protocols.

In Figure 3.1, we show three domains of NC architectural design. The domain clearly relevant for NC to be designed as a NF is the NC functional domain and we develop this domain in the next section.

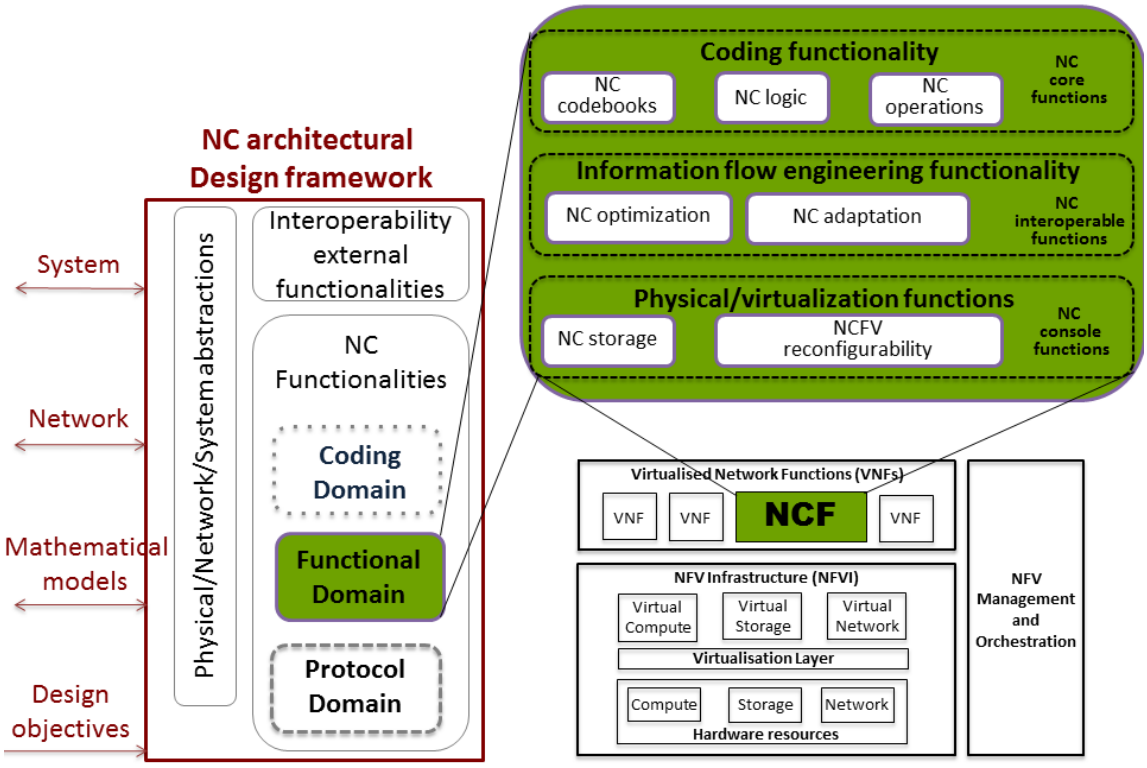

Fig. 3.1 NC architectural design framework and its integration in ETSI NFV architecture in [1] as a toolbox of NC design domains.

3.3 NC Functional Design Domain

Our proposed set of basic NC functionalities are distributed into three hierarchical levels based on their significance, universality and availability. Figure 3.1 denotes common elementary functionalities of NC functional domain [40], which are defined as follows:

- **NC coding functionalities**
  - NC codebooks: elementary encoding/re-encoding/decoding operations, encapsulation/de-encapsulation, adding/removing headers, etc.
  - NC logic: logical interpretation of coding use, coding scheme selection (intra-session/inter-session, coherent/incoherent, file-transfer/streaming, systematic/non-systematic), coding coefficients selection (random/deterministic), etc.
  - NC operations: computation and storage optimization.
- **NC information flow engineering functionalities**
  - NC optimization: resource allocation and optimal allocation of NC parameters possibly differentiating network flows according to design targets and (statistical) status of the networks (congestion, link failures, etc).
  - NC adaptation: control of the time scales for optimization and corresponding reconfiguration across re-encoding nodes across the network.
- **NC physical/virtualization functions**
  - NC Storage: interactions with physical memory.
  - NC Feedback Manager: settings and interaction for acquisition of network statistics feedback.
  - NC Signaling: coordinating signaling parameters and involved encapsulations and/or protocols.

We note that our proposed set of basic functionalities can be easily increased with specialised functionalities and/or future-purpose functionalities.

3.4 Integration of NC into virtualized infrastructures

Interpreting NC as a functionality to the network simply consists in integrating the NC architectural framework described above into existing virtualized architectures.

Given the usual definitions of network functions (e.g. [41]), we define a NCF as follows:

Definition 1. ***Network coding functionality, NCF:*** *is a NF that can be used to transform the payload of information flows to provide a reliable connection service given the computational limitations of the coding nodes.*

In the following, we will illustrate the integration of our proposed NC design as a NF (i.e. NCF) into the NFV architecture and the combined SDN/NFV architecture. In this work, we note that instead of investigating the optimal instantiation of NFs, migration policies of virtualization technology, and showing how they should run along with others e.g., [42, 43], *we focus on the functional design of NCF that can be integrated into current proposals of virtualized architectures*.

3.4.1 Integration of NC into the NFV architecture

As any VNF, we will also need first of all to identify physical networks/systems infrastructure with the physical computing, storage, and network resources that will provide the NCF with processing, storage, and connectivity through virtualization, respectively. Note that every virtual infrastructure will have its corresponding time/space scales and communication/computation resources.

Figure 3.1 shows the NC architectural design framework and how the NC functional domain is integrated in the NFV architecture in [1]. Typical solutions for the deployment of NFV are hypervisors and VMs. VNFs can be realized as an application software running on top of a non-virtualized server by means of an operating system [1]. The architectural integration is proposed here as a toolbox approach. In particular, the set of elementary NC functionalities will enable to tailor the use of NC to engineer the throughput and reliability of multiple information network flows depending on the ultimate service operational intent. The resulting NF will likely operate together with additional virtualized functionalities, which will appropriately be taken care of by the NFV Management and Orchestration (NFV-MANO) (see [1] for further details).

3.4.2 Integration of NC into the combined SDN/NFV architecture

Our NC design can be easily integrated into the combined software-defined and virtualized network architectures. Figure 3.2 illustrates the integration of NC into the combined SDN/NFV architecture [44], which is current trend and fits with our cloud-based architecture. Major benefits of the combined SDN/NFV architecture are as follows. First, NFV can serve SDN by virtualizing and instantiating a SDN controller as a NF at a specific data center in the cloud while on the other hand, SDN serves NFV by providing programmable network

connectivity between VNFs in response to applications and optimized traffic engineering [45]. Second, the integrated architecture allows the flexible control and management of the network/information flows via software in a centralized manner. Third, by the flexibility in management, operational costs can thus be saved by reducing management overhead and time to launch a network service [44].

As illustrated in Figure 3.2, hypervisors are assumed to be available at data centers and coding nodes to support VMs that implement NFs. The NFV-MANO [46] takes charge of managing and orchestrating VNFs under the control of a SDN controller through standard interfaces. A SDN controller e.g., VirNOS, ZENICvDC [44], is responsible for routing and management of NFs via the NFV-MANO [41]. All management functionalities including the SDN controller, NFV-MANO, etc, are considered as VNFs and implemented in data centers while NCF is deployed in distributed nodes along the path.

3.5 Conclusions

In this chapter, we have presented an architectural design for NC with a generic functional design domain. We then illustrate the integration of NC into current proposals of virtualization architectures. Specifically, a toolbox of NC design domains has been identified so that NC can be designed as a NF that provides flow engineering functionalities to the network. Our proposed framework can naturally be tailored for different designs and accommodate additional functionalities.

Finally, the work in this chapter leads to the following publications.

JOURNALS

1. **Tan Do-Duy** and M. A. Vázquez-Castro, "Network Coding Function for Converged Satellite-Cloud Networks", *under review in IEEE Transactions on Aerospace and Electronic Systems (Q1, IF=2.063)*, August 2018.

CONFERENCES

1. **Tan Do-Duy** and M. A. Vázquez-Castro, "Geo-Network Coding Function Virtualization for Reliable Communication over Satellite", in *Proc. IEEE International Conference on Communications (ICC)*, Paris, France, May 2017.

2. **Tan Do-Duy** and M. A. Vázquez-Castro, "Network Coding Function Virtualization", in *Proc. The 17th IEEE International Workshop on Signal Processing Advances in Wireless Communications (SPAWC)*, Edinburgh, UK, July 2016.

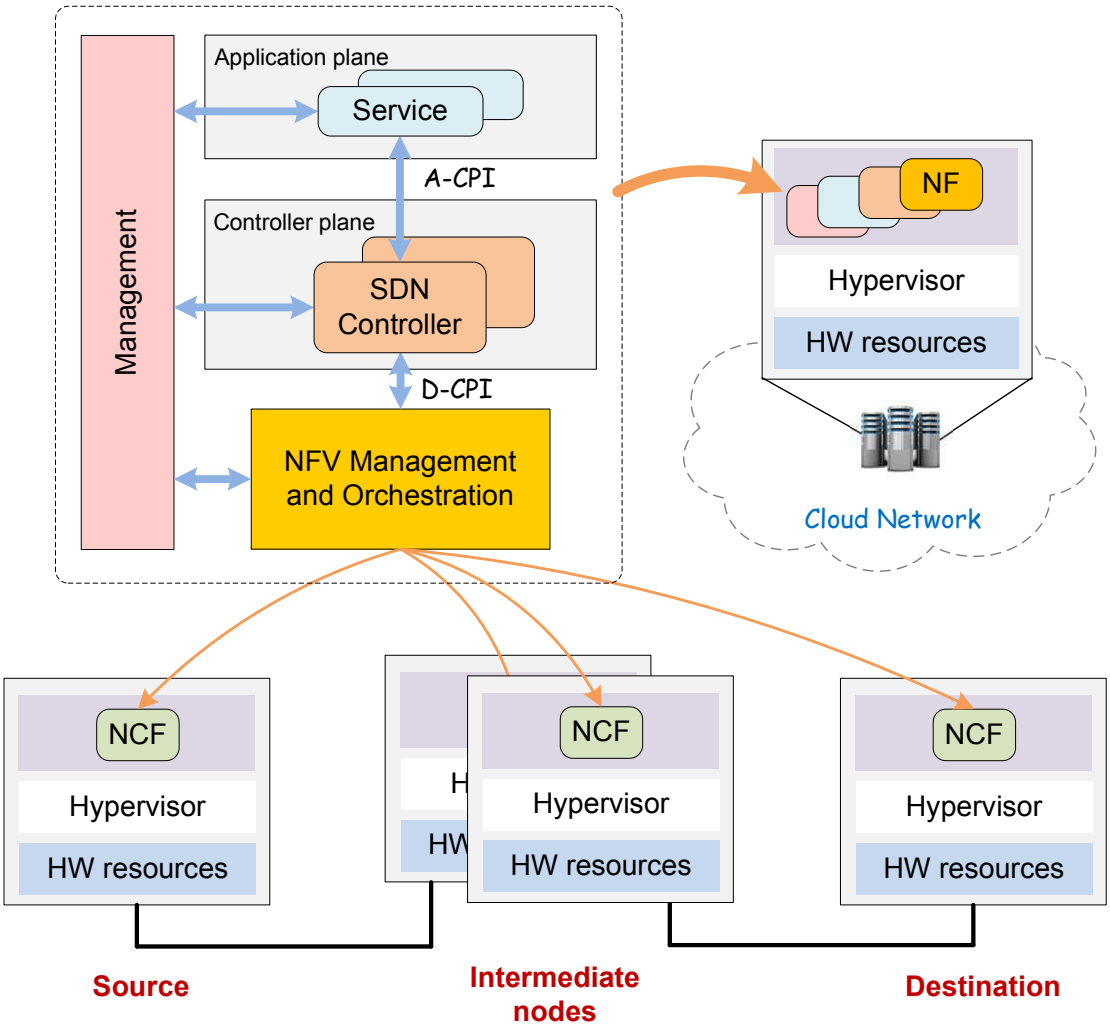

Fig. 3.2 An illustration of the integration of our proposed NC design into the combined SDN/NFV architecture.

Contributions to Project Deliverable Reports: EU H2020 GEO-VISION Project (2015-2017)

1. D2: 2.2 Technical Requirements and 2.3 System Design.
2. D3: 3.1 Research Technology, 3.2 Technology Development, and 3.3 Technology Integration Report.

Contributions to the IRTF

1. M.A. Vázquez-Castro, **Tan Do-Duy**, Simon Romano, Antonia Maria Tulino, "Network Coding Function Virtualization", *IETF Internet-Draft*, May 2017.

Chapter 4

Finite-length Performance Comparison of Linear Network Codes

Our proposed NCF can operate with any packet-level NC scheme. As part of the NC coding domain in the NC architectural design, in this chapter, we will develop a methodology that allows us to evaluate and compare the performance of different NC schemes. We consider a simple, yet common in practice, network model where a source and a destination are connected over a line network of erasure links e.g., relay-aided networks [20, 24].

Linear NC can be roughly classified into two broad classes: random linear NC and structured linear NC. For random linear NC [47, 48], a sender transmits linear combinations of packets with coefficients randomly chosen from a finite field. Re-encoding and decoding can be assumed progressive to minimize packet delay. On the other hand, a structured NC code is any deterministic (algebraic) code [49, 50]. In this case, re-encoding nodes apply decoding and encoding. We use Pascal matrices as exemplary coefficients whose algebraic structure allows the coefficients to be regenerated at the nodes (this reduces overhead).

Existing studies on the practical applications of NC usually assume a fixed size of information source packets [23, 47, 48, 51] or capacity achievability [24, 47] where coding block-length, N, is assumed to tend to infinity, which is not a practical assumption. However, in some practical scenarios, NC is only applicable if the coding block-length is small. Furthermore, the different design constraints (e.g., limits of computational resources at coding nodes [52]) may require different block-length. Therefore, the finite-length coding rates need to be identified for some target PLR requirements given a pre-defined coding block-length. For such cases, in this chapter, we provide a methodology to compute the optimal coding rate of different linear NC schemes as a function of the coding block-length. We evaluate the performance of capacity-achieving codes and coding schemes with scheduling for representative number of links and erasure rates in a line network and obtain the trade-off

between random and structured codes with scheduling. Finally, we provide an example use case applying the considered network codes such that the results clearly show what is the best option in each case.

4.1 Contributions and Structure

4.1.1 Contributions of the Chapter

This chapter presents the contributions that meet Objectives 2 and 3 of this thesis, as defined in Section 1.2:

- **Objective 2: Develop a matricial model that allows us to analyze the corresponding error probabilities of different NC schemes over multi-hop line networks, a simple but common in practice network model.**
  - We model the encoding, re-encoding, and decoding process of different linear coding schemes in matrix notation and corresponding error probabilities over multi-hop line networks. Specifically, we consider random linear capacity-achieving schemes: non-systematic (RLNC) and systematic (SNC) and non-capacity achieving schemes: SNC with packet scheduling (SNC-S) or sliding window (SWNC), and the structured linear schemes based on Pascal matrix: non-systematic (Pascal-NC) and systematic (SPascal-NC).

- **Objective 3: Develop a methodology to compute and evaluate the finite-length performance of different NC schemes which could be selected as the operational NC scheme for the designed NCF.**
  - Towards this objective, we propose a binary searching algorithm to identify optimal coding rate for some specific target packet loss rates given a pre-defined coding block-length. We apply the proposed methodology to compute the optimal finite-length coding rate, achievable rate, and average in-order packet delay for representative number of links and erasure rates. Our simulation results show that for small block-length, the optimal coding rates follow exponential behaviour which could be a challenging issue for the designer of adaptive NC solutions. Further, our methodology is useful to characterize the throughput/delay trade-off between capacity-achieving vs non-capacity achieving schemes in the finite-length regime. Our results aim to guide the network designer to identify the best choice of practical codes and coding rates depending on the user-case.

Specifically, for 4-hop and 10-hop line networks, structured codes with scheduling can provide up to 3.6% and 9.4% gain in achievable rate with coding overhead reduced from 4.9% and 4.5% to 0.067% while the delay increases 18.7% and 152.6% compared to random codes, respectively.

4.1.2 Structure of the Chapter

This chapter is structured as follows. We first present the system model that we consider in this chapter. We model the coding functions and corresponding error probabilities of random and structured linear NC schemes in Section 4.3 and Section 4.4, respectively. In Section 4.5, we propose a searching algorithm to identify the optimal coding rate for given coding block-length and target PLR. Section 4.6 provides simulation results to evaluate the performance of the considered NC schemes using the proposed methodology. Finally, we conclude this chapter in Section 4.7.

4.2 System Model

We study a multi-hop line network $\mathcal{G}$ with $\mathcal{N}$ nodes and $\mathcal{L}$ links connecting a source-destination pair. $\mathcal{D}$ is the set of random variables corresponding to the erasure process associated with each link according to some order. We consider random packet erasure model where each link i is modeled as a memoryless channel erased with probability δ_i $(1 \leq i \leq \mathcal{L})$. We use a unique value δ if all erasure processes are equal.

We assume that a packet stream is produced at the source. Information packets are grouped into equally-sized blocks of length K packets. Such a block is also called a generation. For each generation, we denote $X_{1\times K}$ as K information packets. NC is applied at all nodes so that some target PLR, Pe_0, is guaranteed at the destination node.

Achievable rate at the destination node in $\mathcal{G}$ with NC is defined as $R_{NC}^{\mathcal{N}}(\mathcal{D},\rho) = \rho\Big(1 - P_e^{\mathcal{N}}(\mathcal{D},\rho)\Big)$ with ρ and $P_e^{\mathcal{N}}(\mathcal{D},\rho)$ the coding rate and the PLR at the destination node with NC after decoding, respectively.

4.3 Random Linear Network Coding Schemes

4.3.1 Non-Systematic

For block coding, we consider RLNC and SNC, where information packets are grouped into equally-sized blocks of length K packets. Such a block is also called a generation. For each generation we denote $X_{1\times K}$ as K information packets.

For RLNC, the generator matrix $G \in \mathbb{F}_q^{K\times N}$ consists of elements chosen randomly from the same finite field $\mathbb{F}_q$. Let $X' = XG$ represent N coded packets transmitted by the encoder. Coding rate is $\rho = \frac{K}{N}$. Each intermediate node re-encodes the linear combinations it has received. The decoding is progressive using Gauss-Jordan elimination algorithm.

The PLR for RLNC over a line path $\mathcal{G}$ is given in Eq. (14) of [23] and written here for convenience

$$P_e^{\mathcal{N}}(\mathcal{D},\rho) = 1 - \prod_{i=1}^{\mathcal{L}} \sum_{n=K}^{N} \prod_{j=0}^{K-1} (1-q^{j-n}) Pr(N_i = n), \tag{4.1}$$

where $N_i \sim bin(N, 1-\delta_i)$ are binomial random variables denoting number of coded packets received at re-encoding/decoding node i $(1 \le i \le \mathcal{L})$.

4.3.2 Systematic

The SNC generator matrix is $G = \left[I_K \; C \right]$. It consists of the identity matrix I_K of dimension K and a coefficient matrix $C \in \mathbb{F}_q^{K\times(N-K)}$ with elements randomly chosen from the same finite field $\mathbb{F}_q$. Let $X' = XG$ represent K information (systematic) packets and $N-K$ coded packets transmitted by the encoder. Coding rate is $\rho = \frac{K}{N}$. If a systematic packet is lost, the re-encoder sends a random linear combination of the information packets stored in its buffer [47]. The decoding is progressive using Gauss-Jordan elimination algorithm.

The PLR for SNC over a line path $\mathcal{G}$ is given in Eqs. (15)-(18) of [23] and written here for convenience

$$P_e^{\mathcal{N}}(\mathcal{D},\rho) = 1 - \frac{1}{K} \sum_{z=1}^{K} z Pr(Z_{\mathcal{L}} = z), \tag{4.2}$$

where $Z_{\mathcal{L}}$ is the random number of packets decoded at the decoder.

4.3.3 Systematic with scheduling

The systematic generator $G = \begin{bmatrix} I_K & C \end{bmatrix}$ can be modified to allow variable scheduling of packets (a similar approach is in [48]). Here, we consider the case illustrated in Figure 4.1b, the first $\frac{K}{2}$ information packets of each generation are transmitted first and followed by n_c coded packets which are created by random linear combinations of the first $\frac{K}{2}$ information packets. The last $\frac{K}{2}$ information packets and n_c coded packets are transmitted in sequence. The last n_c coded packets combine all K information packets. In matrix notation, we model SNC with scheduling (SNC-S) as follows. Let $X' = XG$ represent information packets and $2n_c$ coded packets sent by the encoder during $N = K + 2n_c$ timeslots. Coding rate is $\rho = \frac{K}{N}$. The generator matrix is $G = \begin{bmatrix} I_1 & C_1 & I_2 & C_2 \end{bmatrix}$, where

- I_1 : the matrix of size $K \times \frac{K}{2}$, the first $\frac{K}{2}$ columns of the identity matrix of dimension K.
- C_1: the matrix of size $K \times n_c$ where elements of the first $\frac{K}{2}$ rows are chosen randomly from the same $\mathbb{F}_q$ while elements of the last $\frac{K}{2}$ rows are zero.
- I_2 : the matrix of size $K \times \frac{K}{2}$, the last $\frac{K}{2}$ columns of the identity matrix of dimension K.
- C_2: the matrix of size $K \times n_c$ with all elements chosen randomly from the same $\mathbb{F}_q$.

The re-encoder immediately forwards any received information packet to the next node. If a systematic packet is lost, the re-encoder sends a random linear combination of all packets according to the same block stored in its buffer. The decoding is progressive using Gauss-Jordan elimination algorithm.

Due to the lack of analytical expressions, we use simulation results to identify the PLR $P_e^{\mathcal{N}}(\mathcal{D}, \rho)$ for SNC-S.

4.3.4 Sliding Window

We also consider a finite sliding window RLNC scheme (SWNC) [48] (illustrated in Figure 4.1c). The encoder uses an encoding window of size w_e successive information packets. Specifically, the sequence of information packets is divided into groups of size $K_s = \frac{w_e}{2}$. When a new x-th group is generated, the encoding window slides over the sequence of information packets by appending K_s packets of the new group to the end of the window and removing the $(x-2)$-th group from the beginning of the window $(x \geq 3)$. K_s information packets of the new group are sent in consecutive timeslots followed by n_c coded packets created by random combinations of w_e information packets in the encoding window. Coding rate is $\rho = \frac{w_e}{N}$ with $N = w_e + 2n_c$.

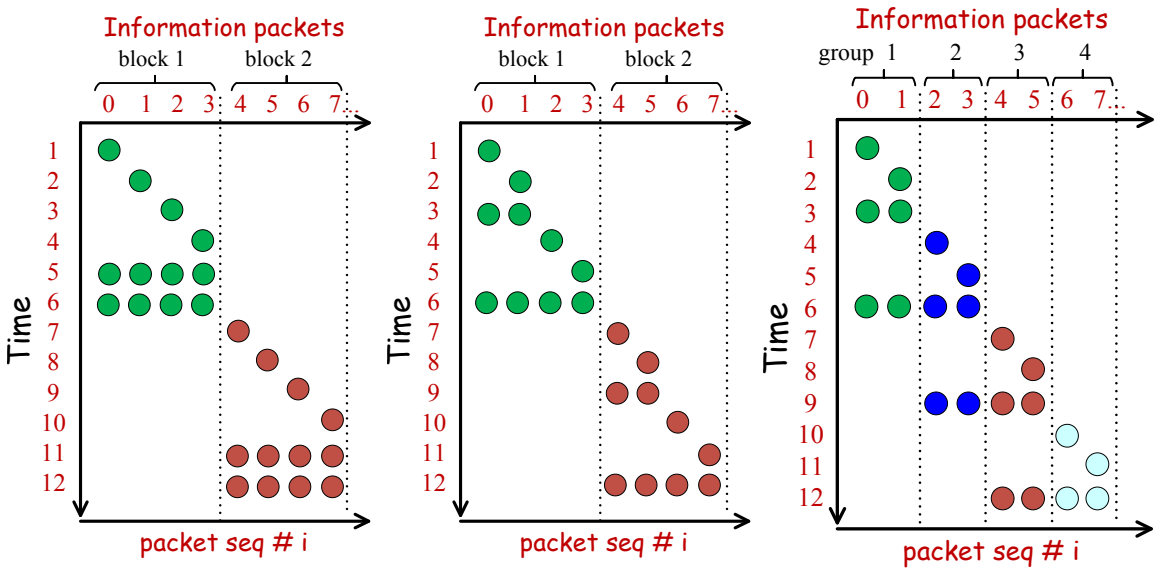

(a) SNC (b) SNC-S (c) SWNC

Fig. 4.1 Illustration of SNC, SNC-S with $K = 4$, SWNC with $w_e = 4$ for $\rho = \frac{2}{3}$. Each single dot represents a uncoded packet whereas multiple dots on a line represent a coded packet.

The generator matrix $G \in \mathbb{F}_q^{w_e \times n_c}$ is a coding coefficient matrix with each element g_i^j denoting a coefficient corresponding to an information packet i-th to obtain the j-th coded packet $(i, j = 0, 1, ...)$. We denote $X' = XG$ as n_c coded packets with $X_{1\times w_e}$ denoting w_e information packets covered by the encoding window. If an information packet with sequence number i is lost, the re-encoder sends a random combination of information packets stored in its buffer with sequence number in range $\left[0, \frac{w_e}{2} - 1\right]$ if $x = 1$ or $\left[(x-2)\frac{w_e}{2}, x\frac{w_e}{2} - 1\right]$ if $x \geq 2$ with $x = \lfloor \frac{i}{w_e/2} \rfloor + 1$. We denote w_d, $w_d \geq w_e$, as the finite decoding window size in number of successive packets e.g. $w_d = w_e$. Iterative Gaussian Elimination can be used to decode packet by packet [48].

Due to the lack of analytical expressions, we use simulation results to identify the PLR $P_e^{\mathcal{N}}(\mathcal{D}, \rho)$ for SWNC.

For illustration, in Figure 4.2, we show numerical values of PLR as a function of ρ for random linear NC schemes on 2-hop and 5-hop line networks.

4.4 Structured Linear Network Coding Schemes

We consider the Pascal matrix P_q over a finite field $\mathbb{F}_q$ as proposed in [49]. Any k columns of P_q are linearly independent and the coefficients follow the structure of binomial coefficients. Hence, when used as a coding coefficient matrix, the Pascal matrix can be easily reproduced

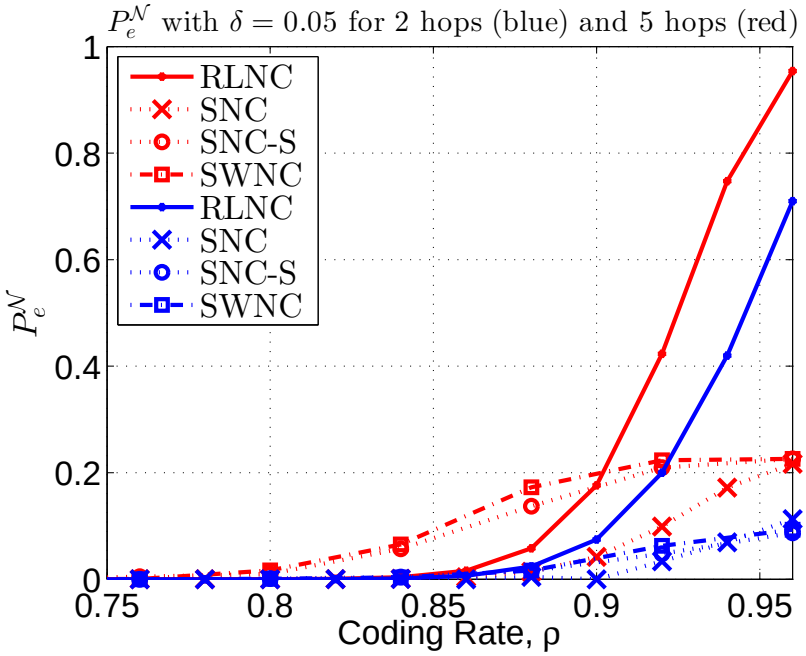

(a) $\delta = 0.05$

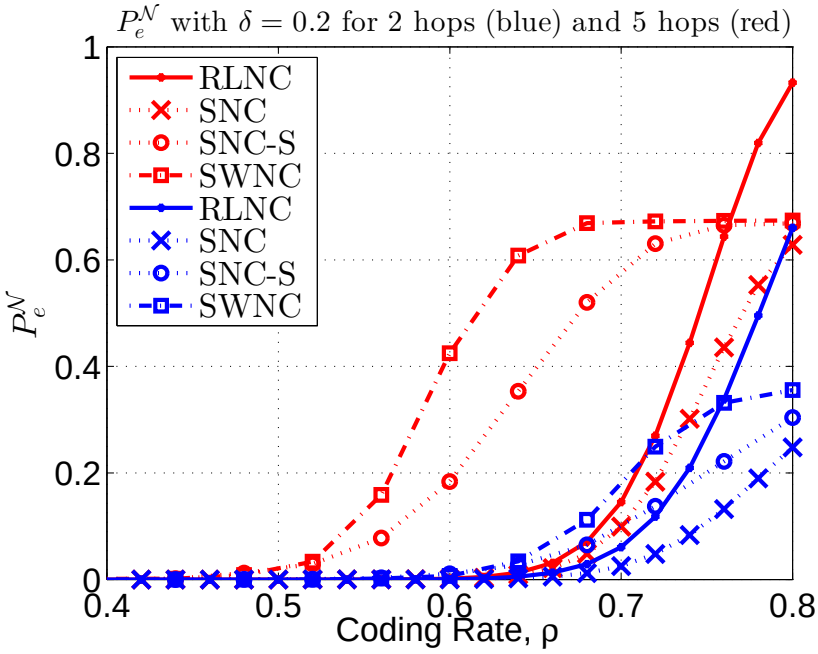

(b) $\delta = 0.2$

Fig. 4.2 PLR at the destination node, $P_e^{\mathcal{N}}(\delta,\rho)$, versus coding rate for the random NC schemes over 2-hop and 5-hop line networks, $N = 50$. PLR for RLNC and SNC is calculated using Eqs. (4.1)-(4.2) while PLR for SNC-S and SWNC is averaged through simulations.

at the nodes [53]. Further, instead of attaching the complete coding coefficients to the corresponding packet, a sender only needs to attach the index, which practically saves bandwidth. The decoding is progressive using Gauss-Jordan elimination algorithm.

4.4.1 Systematic Pascal (PascalNC)

Let $X' = XG$ represent K systematic packets and $N-K$ coded packets transmitted by the encoder. The generator matrix is $G = \Big[I_K\ C\Big]$. It consists of the identity matrix I_K of dimension K and a coefficient matrix $C \in \mathbb{F}_q^{K\times(N-K)}$ extracted from the first K rows and $N-K$ randomly-chosen columns of the Pascal matrix P_q with column index $\geq K$. Coding rate is $\rho = \frac{K}{N}$.

The PLR for PascalNC over a single-hop i in $\mathcal{G}$ $(1 \leq i \leq \mathcal{L})$ can be modified from Eq. (9) of [23] and is rewritten as

$$P_{e_i}(\delta_i, \rho) = 1 - \frac{1}{K}\sum_{z=1}^{K} zPr(Z=z), \tag{4.3}$$

where Z is the random number of packets decoded at the decoding node i. For $x = 1, ..., K-1$,

$$\begin{aligned} Pr(Z=x) &= Pr(U=x)\big(1 - \sum_{c=K-x}^{E} Pr(C=c)\big), \\ Pr(Z=K) &= \sum_{x=0}^{K} Pr(U=x) \sum_{c=K-x}^{E} Pr(C=c), \end{aligned}$$

with $U \sim bin(K, 1-\delta_i)$ and $C \sim bin(N-K, 1-\delta_i)$ the number of uncoded packets and coded packets received at the decoding node i, respectively. Hence, the PLR after decoding at the destination node in $\mathcal{G}$ for PascalNC is given as

$$P_e^{\mathcal{N}}(\mathcal{D}, \rho) = 1 - \prod_{i=1}^{\mathcal{L}} \big(1 - P_{e_i}(\delta_i, \rho)\big). \tag{4.4}$$

4.4.2 Systematic Pascal with Scheduling (PascalNC-S)

The systematic generator $G = \Big[I_K\ C\Big]$ can be modified to allow variable scheduling of packets (a similar approach is in [48]). In particular, let $X' = XG$ represent N packets including K information packets and $N-K$ coded packets sent by the encoder. The first $\lceil \frac{K}{2} \rceil$

information packets of each generation are transmitted first and followed by $n_{c_1} = \lceil \frac{N-K}{2} \rceil$ coded packets which are created by linear combinations of the first $\lceil \frac{K}{2} \rceil$ information packets. The last $K - \lceil \frac{K}{2} \rceil$ information packets and $n_{c_2} = N - K - n_{c_1}$ coded packets combining all K information packets are transmitted in sequence. Coding rate is $\rho = \frac{K}{N}$. Hence, the PascalNC-S generator matrix is $G = \left[I_1 \; C_1 \; I_2 \; C_2 \right]$, where

- I_1 : the matrix of size $K \times \lceil \frac{K}{2} \rceil$, the first $\lceil \frac{K}{2} \rceil$ columns of the identity matrix of dimension K.
- C_1: the matrix of size $K \times n_{c_1}$ where elements of the first $\lceil \frac{K}{2} \rceil$ rows are extracted from the first $\lceil \frac{K}{2} \rceil$ rows and n_{c_1} randomly-chosen columns of the Pascal matrix P_q with index $\geq \lceil \frac{K}{2} \rceil$ while the remaining elements are zero.
- I_2 : the matrix of size $K \times \left(K - \lceil \frac{K}{2} \rceil \right)$, the last $K - \lceil \frac{K}{2} \rceil$ columns of the identity matrix of dimension K.
- C_2: the matrix of size $K \times n_{c_2}$ with elements extracted from the first K rows and n_{c_2} randomly-chosen columns of the Pascal matrix P_q with column index $\geq K$.

Due to the lack of analytical expressions, we use simulation results to identify the PLR $P_e^{\mathcal{N}}(\mathcal{D}, \rho)$ for PascalNC-S.

For illustration, in Figure 4.3, we show numerical values of PLR at the destination node, $P_e^{\mathcal{N}}(\delta, \rho)$, as a function of ρ for the considered NC schemes on 2-hop and 5-hop line networks. The figure shows the gap in PLR for the structured and random NC schemes which increases with the number of links since with the structured schemes, decoding is performed at all intermediate nodes.

4.5 Optimal Finite Length Coding Rate

We now investigate how to choose an optimal coding rate, ρ^*, given a particular block-length N for some target Pe_0 at the destination node in $\mathcal{G}$ with $\mathcal{L}$ links (hops).

We employ the bounds of PLR to show its monotonic property so that a searching algorithm is sufficient to identify ρ^* for the random linear NC schemes given N and Pe_0. We consider RLNC as an illustration due to the similar properties of PLR versus ρ for the considered NC schemes given a specific N [23, 48].

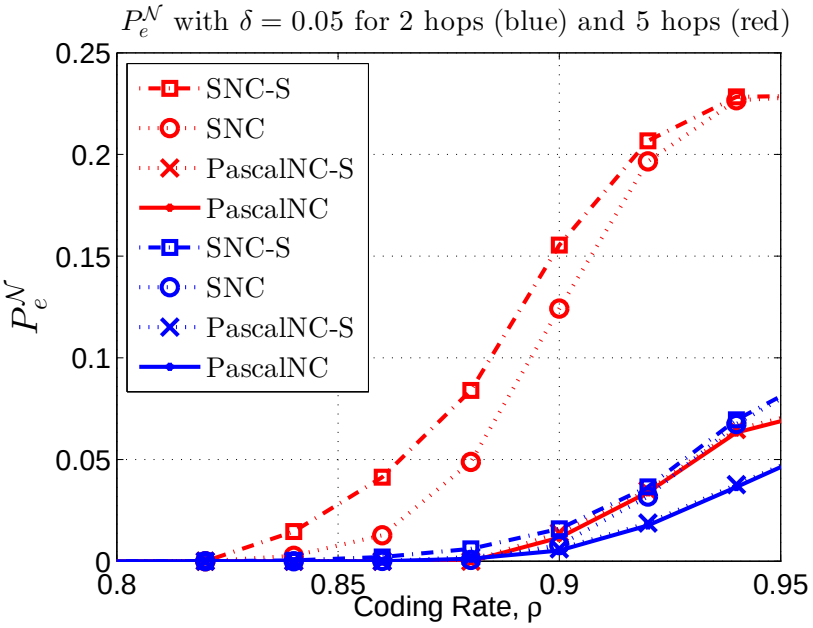

(a) $\delta = 0.05$

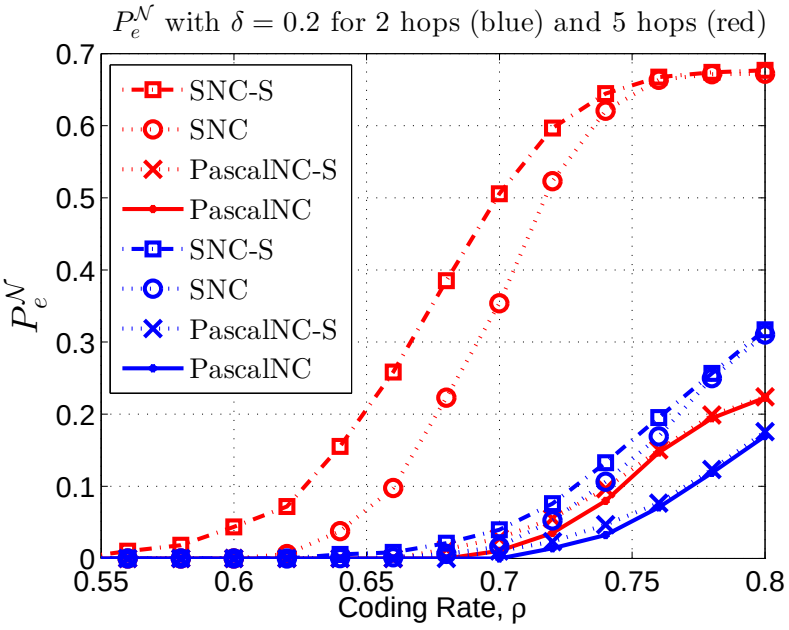

(b) $\delta = 0.2$

Fig. 4.3 PLR at the destination node, $P_e^{\mathcal{N}}(.)$, versus coding rate for the structured and random NC schemes over 2-hop and 5-hop line networks, $N = 100$. PLR for PascalNC is calculated using Eq. (4.4) while PLR for the other schemes is averaged through simulations.

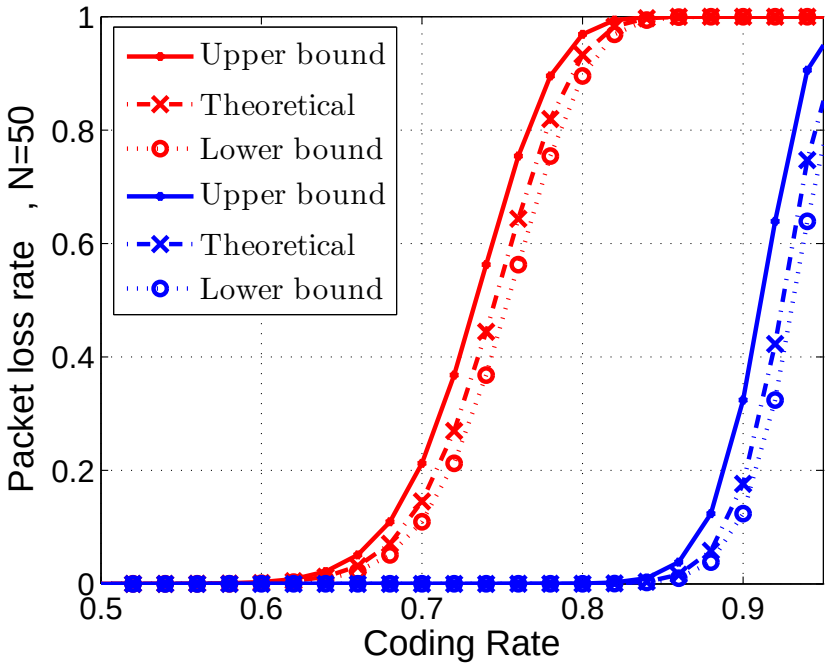

Fig. 4.4 PLR for RLNC obtained from Eq. (4.1) (theoretical) and its bounds over 5-hop line networks with $\delta = 0.05$ (blue) and $\delta = 0.2$ (red).

Proposition 1. *PLR for RLNC can be bounded as*

$$1-\prod_{i=1}^{\mathcal{L}} 1-C_{p_i}\big(K-1\big) \leq P_e^{\mathcal{N}}(\mathcal{D},\rho) \leq 1-\prod_{i=1}^{\mathcal{L}} 1-C_{p_i}\big(K\big), \tag{4.5}$$

where $C_{p_i}(m) = \phi\left(sgn(\frac{m}{N}-p_i)\sqrt{2NH(\frac{m}{N},p_i)}\right)$, *with* $sgn(x)$ *be the usual signum function with argument* x, $\phi(y)$ *be the distribution function of a standard normal variable with argument* y, $H(x,p_i) = xln\frac{x}{p_i} + (1-x)ln\frac{1-x}{1-p_i}$, $sgn(x) = \frac{x}{|x|}$, $p_i = 1-\delta_i$.

Proof. For a sufficiently large field size q, PLR for RLNC given in Eq. (4.1) can be rewritten as $P_e^{\mathcal{N}}(\mathcal{D},\rho) = 1-\prod_{i=1}^{\mathcal{L}}\sum_{n=K}^{N} Pr(N_i=n)$.

Zubkov et al. [54] proved that for $1 \leq m \leq N$, $C_{p_i}(m) \leq \sum_{n=0}^{m} Pr(N_i=n) \leq C_{p_i}(m+1)$. Hence, we obtain the bound of PLR for RLNC as in Eq. (4.5). □

Figure 4.4 shows the theoretical PLR for RLNC obtained from Eq. (4.1) and its bounds versus coding rate over 5-hop line networks.

Proposition 2. *For given* N *and* Pe_0, *a binary searching algorithm is sufficient to identify* ρ^* *and converges in* $k' = \lceil log_2(|\Psi_N|-1)\rceil$ *iterations with* Ψ_N *the set of coding rates available for searching.*

Proof. We consider the upper bound of PLR for RLNC proposed in Proposition 1, given as

$$P_e^{\mathcal{N}}(\mathcal{D},\rho) = 1 - \prod_{i=1}^{\mathcal{L}} 1 - \phi\left(sgn(\rho - p_i)\sqrt{2NH(\rho,p_i)}\right). \tag{4.6}$$

Let consider functions $z = H(\rho,p_i)$, $y = sgn(\rho-p_i)\sqrt{2NH(\rho,p_i)}$, and $f(\rho) = 1 - \prod_{i=1}^{\mathcal{L}} 1 - \phi\Big(y(\rho)\Big)$. We obtain $z^{'} = \frac{dz}{d\rho} = ln\frac{\rho(1-p_i)}{(1-\rho)p_i} = 0$ at $\rho = p_i$. For example, for $p_i = 0.8, \rho = 0.5$, $z^{'} = ln(0.25) < 0$. Hence, z decreases with $\rho \in (0,p_i)$ and then increases with $\rho \in (p_i,1)$. Further, for $\rho < p_i$, $sgn(\rho - p_i) = -1$. Hence, y increases with $0 < \rho < 1$. Thus, $f(\rho)$ is a non-decreasing function of ρ. For some N, $f(\frac{K}{N})$ is also a non-decreasing function of K. Hence, assume $K = N\rho$, a unique ρ^* can be identified by a binary searching algorithms [55] so that $P_e^{\mathcal{N}}(\mathcal{D},\rho^*) \simeq Pe_0$.

To prove the convergence of a binary searching algorithm, we define $g(\rho) = P_e^{\mathcal{N}}(\mathcal{D},\rho) - Pe_0$ and find the number of iterations until achieving the root of $g(\rho) = 0$ [56]. We consider a set Ψ_N of coding rate with $\rho[i] = i\rho_0$ $(1 \le i \le |\Psi_N|)$ (unit step ρ_0). For a binary algorithm, we denote $first$ and $last$ as the indices of the first and the last coding rate of searching window in Ψ_N and $mid = \lfloor \frac{first+last}{2} \rfloor$. We also denote a and b as the initial value of $first$ and $last$, respectively. Generally, suppose that we have $\big[\rho[a],\rho[b]\big]$ such that $g(\rho[a]) < 0$ and $g(\rho[b]) > 0$. Since $g(\rho)$ is continuous and non-decreasing on $\big[\rho[a],\rho[b]\big]$, the intermediate value theorem shows that $g(\rho) = 0$ has one root on the interval.

Let a_k, b_k, and c_k denote the k^{th} computed values of $first$, $last$, and mid, respectively. Hence, we have $b_{k+1} - a_{k+1} = \lfloor \frac{b_k - a_k}{2} \rfloor$ and $b_k - a_k = \lfloor \frac{b-a}{2^{k-1}} \rfloor$ $(k \ge 1)$. Since the index α w.r.t. the best coding rate (such that $g(\rho[\alpha]) \simeq 0$) $\alpha \in [a_k,c_k]$ or $\alpha \in [c_k,b_k]$, we can write $|\alpha - c_k| \le \lfloor \frac{b_k-a_k}{2} \rfloor = \lfloor \frac{b-a}{2^k} \rfloor$ and $\big|\rho[\alpha] - \rho[c_k]\big| \le \lfloor \frac{b-a}{2^k} \rfloor \rho_0$. We compute the maximum number of iterations k' needed to achieve ρ^* as follows. Algorithm 1 identifies $\rho^* = \rho[\alpha]$ i.e., $\big|\rho[\alpha] - \rho[c_{k'}]\big| = 0$. This is satisfied if $\lfloor \frac{b-a}{2^{k'}} \rfloor \rho_0 = 0$. Hence, the searching algorithm converges after a maximum number of $k' = \lceil log_2(b-a) \rceil = \lceil log_2(|\Psi_N| - 1) \rceil$ iterations. □

Hence, we propose an algorithm based on the binary searching algorithm in [55], which is summarized in Algorithm 1. By assuming $K = \lceil N\rho \rceil$ (or $w_e = \lceil N\rho \rceil$), PLR for a specific NC scheme is considered as a function of ρ and $\mathcal{L}$ and can be calculated using theoretical expressions or simulations. ρ^* is the maximum ρ that $P_e^{\mathcal{N}}(\mathcal{D},\rho) \le Pe_0$ holds. We denote Ψ_N as the set of coding rates available for searching. Then, the complexity of the proposed searching algorithm is $\mathcal{O}(log_2|\Psi_N|)$ [55]. Note that the complexity of simulations in the proposed algorithm is not an issue since one can perform the algorithm only once and then keep the values as a table.

Algorithm 1 The proposed searching algorithm to identify ρ^*.

Initialize
  Set $\mathcal{D}$, $\mathcal{N}$, N, Pe_0, $K = \lceil N\rho \rceil$ ($w_e = \lceil N\rho \rceil$)
  For a set Ψ_N of coding rate, $\rho[i] = i\rho_0$, $1 \leq i \leq |\Psi_N|$ (unit step ρ_0 e.g., $\rho_0 = \frac{1}{N}$)
  Set $first = 1$, $last = |\Psi_N|$, $\rho^* = \emptyset$
while $(first < last)$ {
  Set $mid = \lfloor \frac{first+last}{2} \rfloor$
  Calculate $P_e^{\mathcal{N}}(\mathcal{D}, \rho[mid])$ using theoretical expressions or simulation
  if $mid = first$ **then**
    if $P_e^{\mathcal{N}}(\mathcal{D}, \rho[mid]) \leq Pe_0$ **then**
      Set $\rho^* = \rho[mid]$
    break
  else if $P_e^{\mathcal{N}}(\mathcal{D}, \rho[mid]) \leq Pe_0$ **then**
    Set $first = mid$
    Set $\rho^* = \rho[mid]$
  else Set $last = mid$ }
Return ρ^*

4.6 Performance Evaluation

4.6.1 Simulation Settings

In this subsection, we evaluate the finite-length performance of the considered NC schemes with $Pe_0 = 10^{-6}$ and $Pe_0 = 10^{-3}$ representing the quasi-error-free channel and delay-constrained applications [57], respectively. We assume packet length is $L = 1500$ bytes ($m = 8$, $q = 2^8$). We set the unit step $\rho_0 = \frac{1}{N}$ and $|\Psi_N| = N - 1$. We consider $\delta = 0.05$ and $\delta = 0.2$ representing 802.11 wireless links [58] and transmission scenarios with links having light rainfall [47], respectively. Optimal coding rate, ρ^*, given block-length N and Pe_0 is obtained from Algorithm 1 using simulations in Matlab. We note that Algorithm 1 can operate with any target PLR and erasure rates. The capacity of the topology is the min-cut of the networks which is given by $\min_{1 \leq i \leq \mathcal{L}} \left(1 - \delta_i\right)$.

4.6.2 Optimal Coding Rate

In Figure 4.5, we show the optimal coding rate, ρ^*, obtained from Algorithm 1 versus block-length over 2-hop and 5-hop line networks for $Pe_0 = 10^{-6}$.

Major conclusions can be inferred as follows:

- For the same N and $\mathcal{D}$, the larger the number of links $\mathcal{L}$, the lower the optimal coding rate [23]. The reason is that as observed from Eq. (4.6), for any ρ, $\prod_{i=1}^{\mathcal{L}} 1 -$

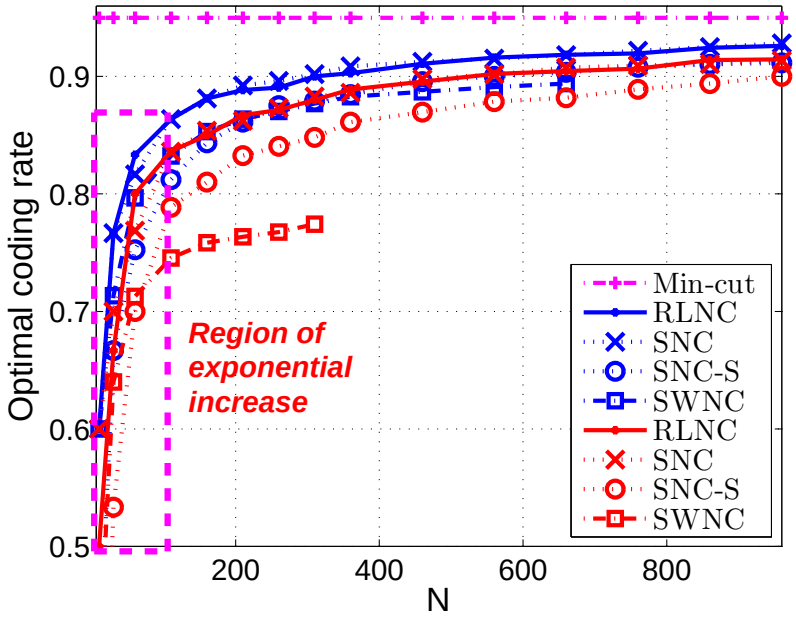

(a) $\delta = 0.05$

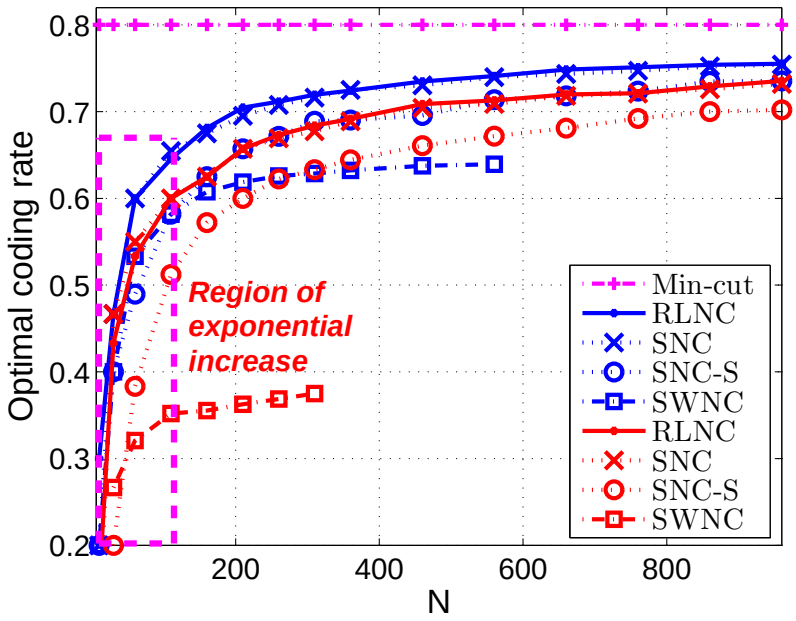

(b) $\delta = 0.2$

Fig. 4.5 Optimal coding rate, ρ^*, versus N for different network codes over 2-hop and 5-hop line networks with $\delta = 0.05$ and $\delta = 0.2$, respectively, for $Pe_0 = 10^{-6}$ (blue: $\mathcal{L} = 2$ hops, red: $\mathcal{L} = 5$ hops).

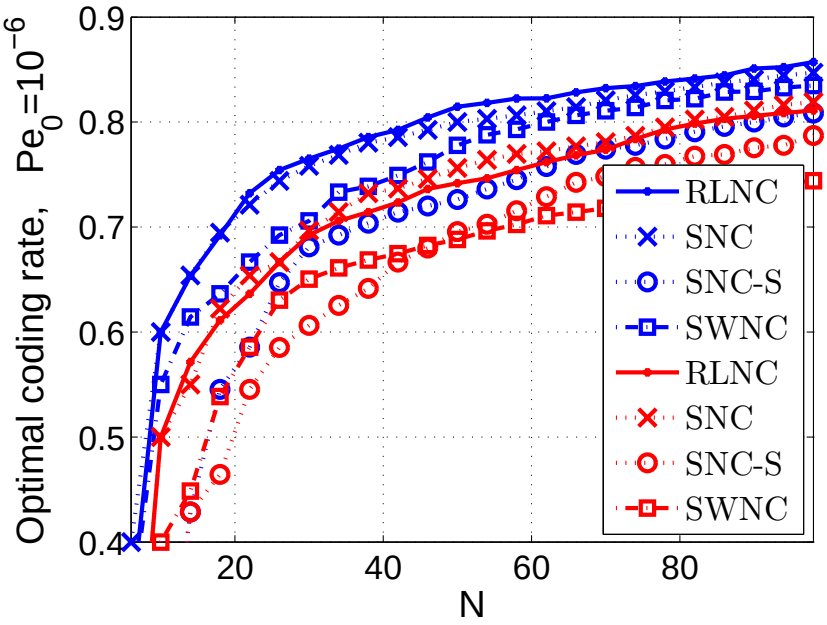

(a) $\delta = 0.05$

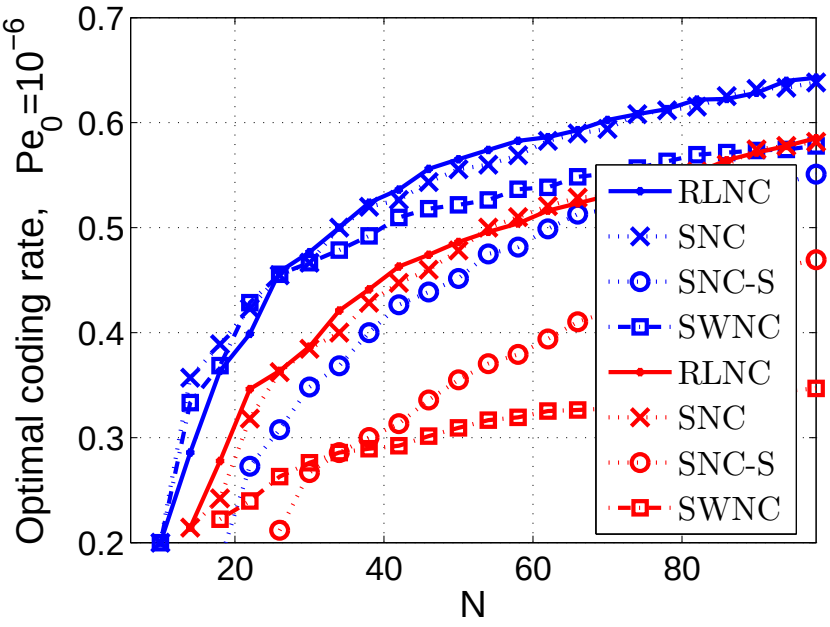

(b) $\delta = 0.2$

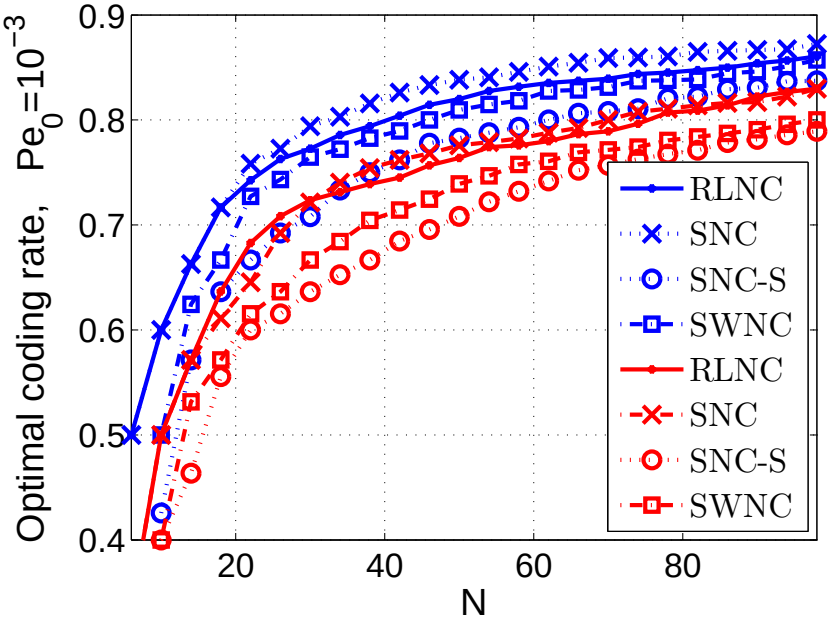

(c) $\delta = 0.05$

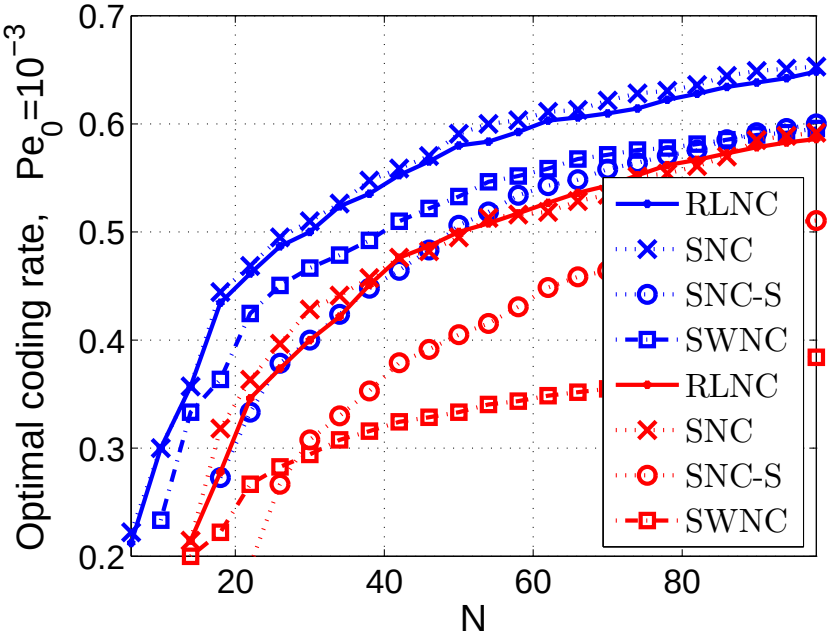

(d) $\delta = 0.2$

Fig. 4.6 Optimal coding rate in the region of exponential increase ($N \leq 100$) with $\delta = 0.05$ and $\delta = 0.2$ for $Pe_0 = 10^{-6}$ (Fig. 4.6a-4.6b) and $Pe_0 = 10^{-3}$ (Fig. 4.6c-4.6d) (blue: $\mathcal{L} = 2$ hops, red: $\mathcal{L} = 5$ hops).

$\phi\left(sgn(\rho - p_i)\sqrt{2NH(\rho, p_i)}\right)$ reduces with number of links $(0 \leq \phi(.) \leq 1)$. Hence, $P_e^N(.)$ increases with $\mathcal{L}$.

- The figure shows the region of exponential coding rate increase for $N \leq 100$. This indicates that when the coding block-length needs to be small, the optimal coding rate undergoes exponential behaviour. Therefore, adaptive coding policies require careful design. Specifically, we depict the region of exponential increase with $Pe_0 = 10^{-6}$ and $Pe_0 = 10^{-3}$ in Figure 4.6. The curves follow the saturating exponential function $\rho^*(N) = c - ae^{-bN}$. Hence, the slope as a function of N can be given by $f(N) = (\rho^*(N))' = abe^{-bN}$, which shows the decrease of slope with block-length.

- As expected, for the same N and $\mathcal{D}$, the lower the Pe_0, the lower the ρ^*. Moreover, the impact of the lost packets of the immediately preceding group on the SWNC decoding process increases with erasure rates, number of links, and number of information packets in each group. Thus, when N is large enough, ρ^* for SWNC is lower than that of SNC-S.

4.6.3 Optimal Achievable Rate

In Figure 4.7, we show the optimal achievable rate at the destination node in $\mathcal{G}$ with different linear NC schemes over 2-hop and 5-hop line networks.

Main conclusions can be inferred as follows:

- For small block-length, the optimal achievable rate follows an exponential behavior. Further, the lower the Pe_0, the lower the optimal achievable rate.

- For the same number of links and erasure rates, the optimal achievable rate with PascalNC outperforms that of the other schemes due to the effect of decoding and encoding at intermediate nodes.

- Due to the size of the Pascal matrix P_q, PascalNC and PascalNC-S cannot work with an arbitrarily large block-length. In contrast, SNC and SNC-S can work with any block-length, which only depends on design constraints e.g., computational resources at the nodes or packet delay constraints of network services.

4.6.4 Average In-order Packet Delay

We use simulations to evaluate average in-order packet delay. For a stream of $|\mathcal{S}|$ information packets, let τ_j denote the difference between the time a packet $j \in \mathcal{S}$ is transmitted by

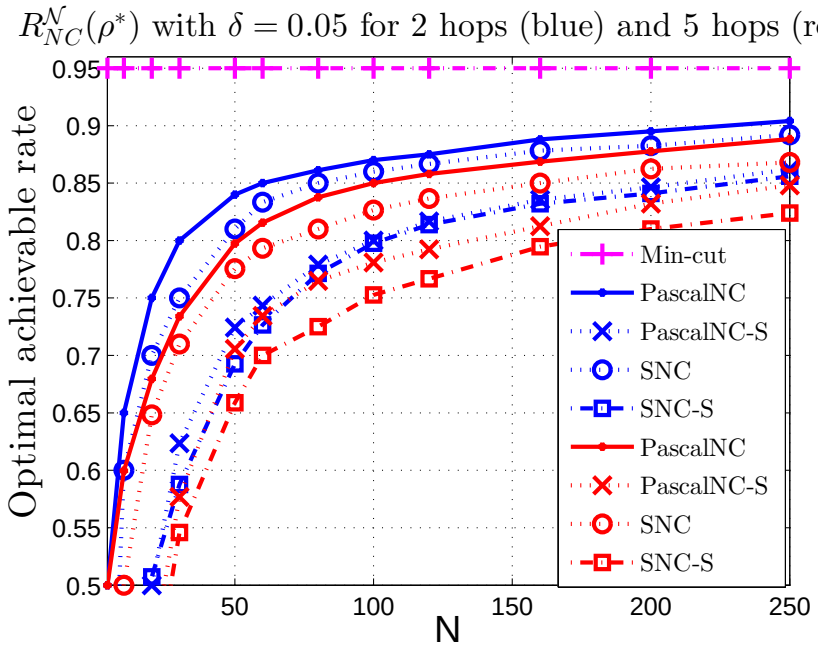

(a) $\delta = 0.05$

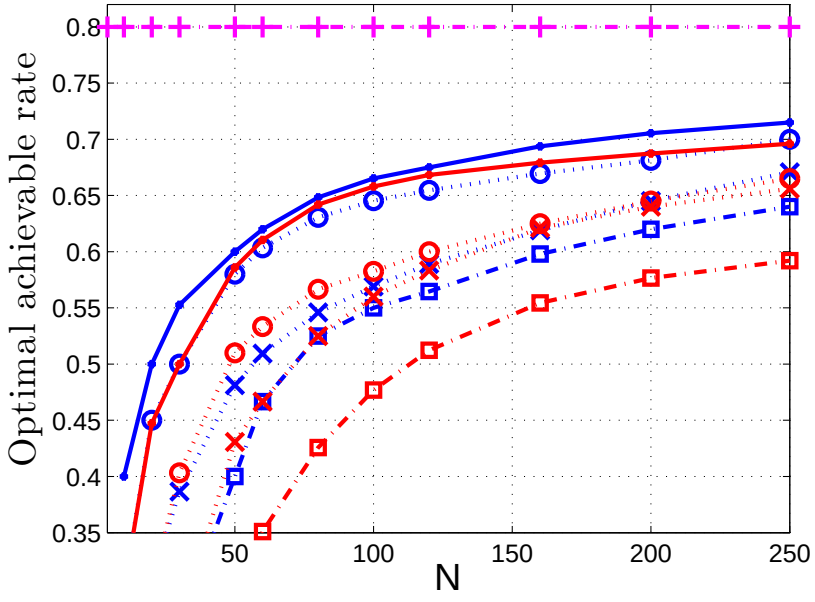

(b) $\delta = 0.2$

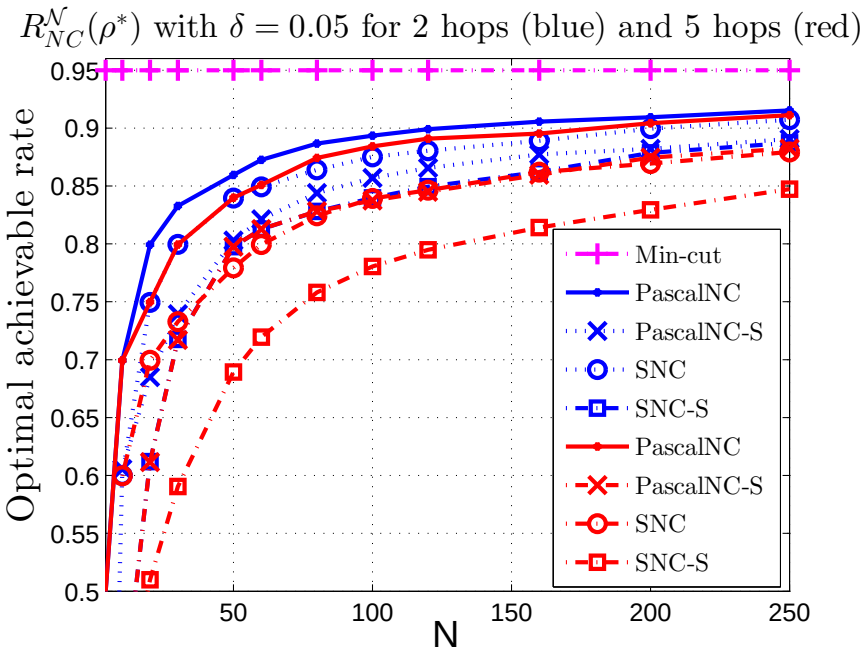

(c) $\delta = 0.05$

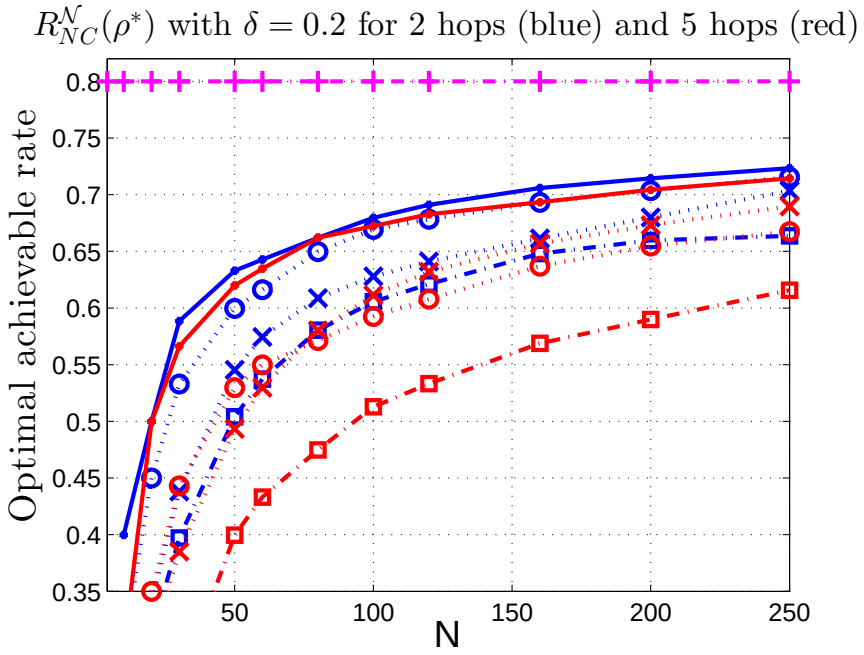

(d) $\delta = 0.2$

Fig. 4.7 Optimal achievable rate at the destination node, $R_{NC}^{\mathcal{N}}(\delta, \rho^*)$, versus N for different linear NC schemes over 2-hop and 5-hop line networks with $Pe_0 = 10^{-6}$ (Fig. 4.7a-4.7b) and $Pe_0 = 10^{-3}$ (Fig. 4.7c-4.7d).

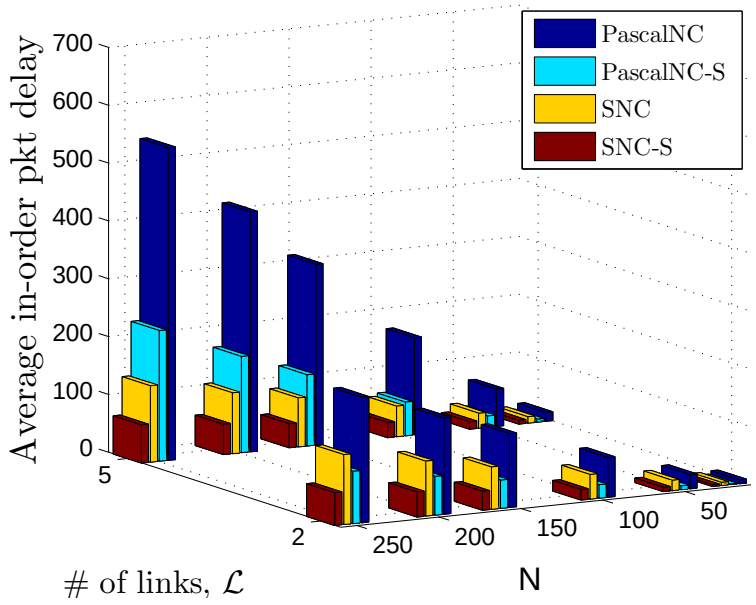

(a) $\delta = 0.05$

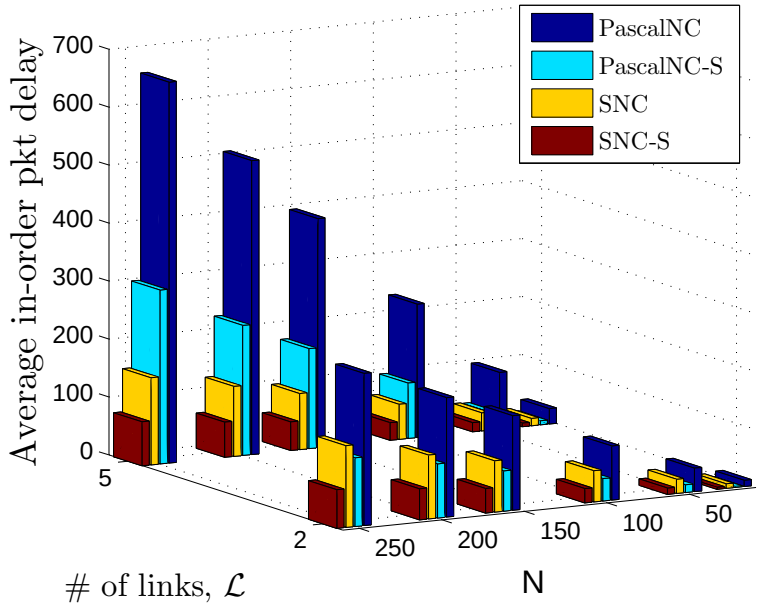

(b) $\delta = 0.2$

Fig. 4.8 Average in-order packet delay at the destination, $\tau_{nc}^{\mathcal{N}}(\delta, \rho^*)$ (in timeslots), vs. N for different NC schemes over 2-hop and 5-hop line networks, with $Pe_0 = 10^{-3}$.

the source and the time that it is delivered in-order at the destination. For the set $\mathcal{S}^* \subset \mathcal{S}$ packets delivered successfully, average in-order packet delay at the destination is computed as $\tau_{nc}^{\mathcal{N}}(\mathcal{D},\rho) = \frac{\Sigma_{j=1}^{|\mathcal{S}^*|}\tau_j}{|\mathcal{S}^*|}$ (in timeslots).

Figure 4.8 shows average in-order packet delay w.r.t. the optimal coding rate versus N and $\mathcal{L}$ for different NC schemes.

Conclusive results are as follows:

- Average in-order packet delay increases linearly with N and $\mathcal{L}$. In the following, we provide a justification using a bound of average packet delay. We consider a multi-hop line path $\mathcal{G}$ with $\mathcal{N}$ nodes and $\mathcal{L}$ links. Given each block of K information packets generated at the source, the expected number of timeslots needed to deliver K packets to the destination in $\mathcal{G}$ $(n = \mathcal{N})$ is bounded as [59]

$$\tau_{nc}^{\mathcal{N}} \leq \frac{K}{1 - \max\limits_{1\leq i\leq \mathcal{L}} \delta_i} + \sum_{i=1, i\neq v}^{\mathcal{L}} \frac{\delta_v}{\delta_v - \delta_i}, \tag{4.7}$$

  with $\delta_v \coloneqq \max\limits_{1\leq i\leq \mathcal{L}} \delta_i$, $\delta_i < \delta_v \; \forall i \neq v$. We assume a $v^{'}$-th link with $\delta_{v'} \coloneqq \max\limits_{1\leq j\leq \mathcal{L}, \forall j\neq v} \delta_j$, $\delta_j \leq \delta_{v'} < \delta_v$. Hence, we write

$$\sum_{i=1, i\neq v}^{\mathcal{L}} \frac{\delta_v}{\delta_v - \delta_i} = \sum_{i=1, i\neq v}^{\mathcal{L}} \frac{1}{1 - \frac{\delta_i}{\delta_v}} \leq \Big(\mathcal{L} - 1\Big) \frac{1}{1 - \frac{\delta_{v'}}{\delta_v}}. \tag{4.8}$$

  By replacing Ineq. (4.8) into Ineq. (4.7), the resulting equation shows that the average in-order delay increases linearly with K and $\mathcal{L}$. Further, as showed in Section 4.6.2, approximately the optimal achievable rate increases linearly when N is large enough e.g. $N > 100$. Therefore, $\frac{K_1}{K_2}\frac{N_2}{N_1} \approx constant$ given a target PLR Pe_0. Hence, the average delay increases linearly with N.

- As expected, average in-order packet delay with PascalNC and PascalNC-S is notably higher than that of SNC and SNC-S, respectively, due to the decoding and encoding process at intermediate nodes. This shows the rate-delay tradeoff as the structured schemes obtain higher achievable rate while incurring high delay, which reduces with the random schemes.

4.6.5 An Example Use Case

We now provide an example use case applying both codes to clearly show what is the best option in each case. We study a device-to-device (D2D) communication network for emergency scenarios [20] where a source transmits video packets to a destination over a line network. We assume that each node (e.g. smartphones) transmits a packet in a timeslot. The flow bit-rate is 2.5 Mbps. Hence, the slot duration is $\frac{L*8}{2500} = 4.8$ ms, which is the same for all timeslots used by all nodes. We only focus on delay caused by network codes and thus ignore the buffering delay at the nodes and transmission delay along D2D links.

In Figure 4.9, we show the optimal achievable rate and average in-order packet delay (in ms) at the destination, and coding overhead with different NC schemes, respectively. We consider different number of links between the source-destination pair with $\delta = 0.1$ representing 802.11 wireless links. We define coding overhead (in %) as the amount of symbols in a packet needed by the network code to signal coding coefficients. Specifically, for PascalNC-S, 1 symbol is needed to signal coding coefficients. For SNC and SNC-S, $\mathcal{L}-1$ symbols are invested in sending random seeds for generating pseudo-random coding coefficients (SEED) while K symbols are invested in sending coding coefficients when random seeds are not used (COEF).

The results indicate that PascalNC-S can provide significant improvements on the achievable rate compared to the random codes, however, it incurs high packet delay. For example, for $\mathcal{L} = 4$ and $\mathcal{L} = 10$, the achievable rate gain with PascalNC-S can reach some 3.6% and 9.4% while the delay increase is 18.7% and 152.6% compared to SNC, respectively. Accordingly, coding overhead reduces from 0.2% and 0.6% to 0.067% when random seeds are used and from 4.9% and 4.5% to 0.067% when random seeds are not used. Hence, the selection of an appropriate network code should take into account both the gain in achievable rate and delay requirements of network services.

From the results in Figure 4.9, in Table 4.1, we show an example for the selection of network codes such that the achievable rate is maximized while PLR and packet delay do not exceed some pre-defined thresholds. We assume different values of delay constraints for video services over D2D networks [20, 57]. We see that for low delay constraints e.g. 200 ms, SNC and SNC-S are the best options for low and high number of links between the source and the destination, respectively. On the other hand, for high delay constraints e.g. 1000 ms, PascalNC-S should be chosen for both low and high number of links.

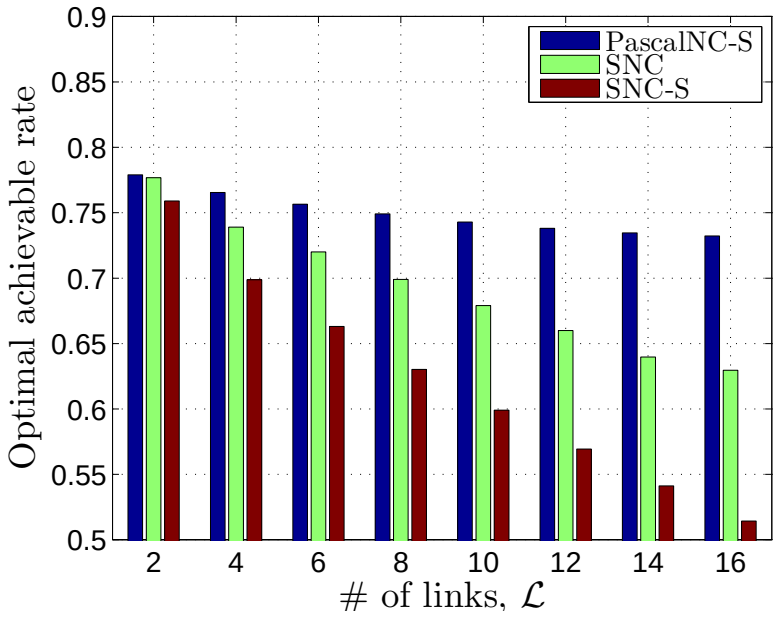

(a) Achievable rate

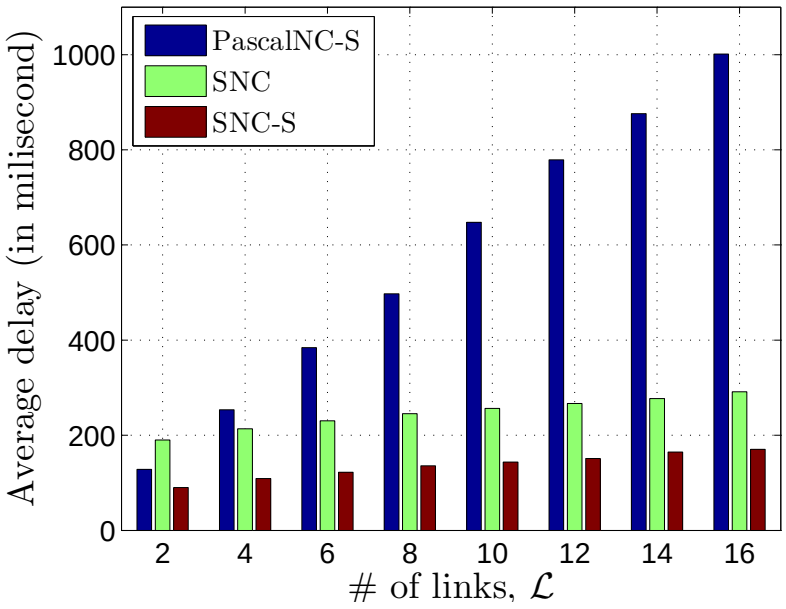

(b) Packet Delay

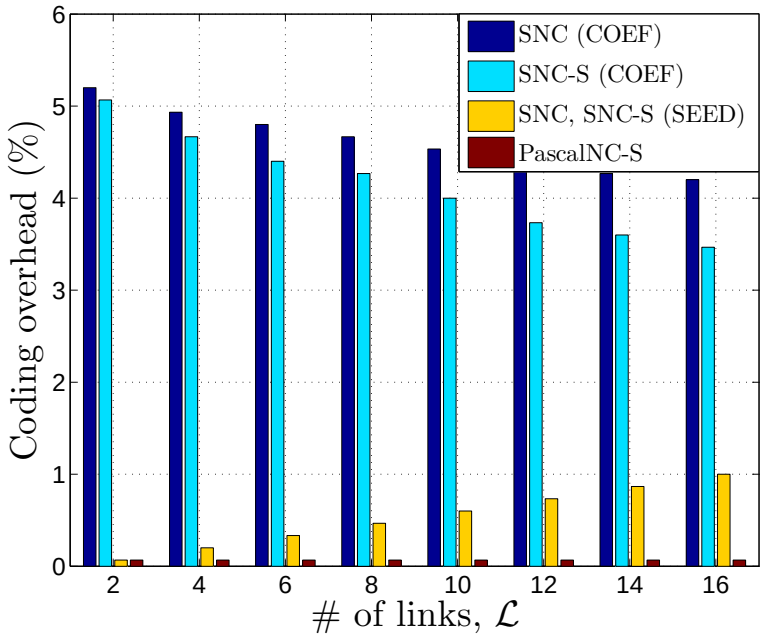

(c) Coding Overhead

Fig. 4.9 Optimal achievable rate and average in-order packet delay (in ms) at the destination, and coding overhead for different number of links between a source-destination pair, with $\delta = 0.1$, $N = 100$, $Pe_0 = 10^{-3}$.

Network code selected		**# of links btw the source & destination**		
		2-4	**5-8**	**> 8**
Delay constraint (milisec)	**200**	SNC	SNC-S	SNC-S
	500	PascalNC-S	PascalNC-S	SNC
	1000	PascalNC-S	PascalNC-S	PascalNC-S

Table 4.1 The optimal selection of network codes for the use case w.r.t. different number of links between the source-destination pair and delay constraints, $Pe_0 = 10^{-3}$.

4.7 Conclusions

In this chapter, we have developed a matricial model that allows us to analyze the corresponding error probabilities of different NC schemes over multi-hop line networks. Then, we have proposed a methodology to compute the optimal finite-length coding rate for linear NC schemes over a line network. By applying the proposed method, we have modeled the exponential increase of the optimal coding rate with block-length, which reveals the difference between capacity-achieving schemes and non-achieving schemes. We have then compared the performance of the Pascal matrices-based structured and random linear NC schemes with optimal finite-length coding rates over multi-hop line networks. The results reveal the pros and cons of the structured and random linear NC schemes in terms of achievable rate, coding overhead, and packet delay for representative erasure rates, target PLRs, and number of links. Furthermore, we have applied the considered network codes in an example use case to show the best choice in each case.

Finally, the work in this chapter leads to the following publications.

JOURNALS

1. **Tan Do-Duy**, P. Saxena, and M. A. Vázquez-Castro, "Finite-length Performance Comparison of Network Codes using Random vs Pascal Matrices", *under review in IEEE Wireless Communications Letters (Q1, IF=3.096)*, August 2018.

2. **Tan Do-Duy** and M. A. Vázquez-Castro, "Finite-length Network Coding for Integrated MANETs-Satellite Networks", *under review in Elsevier Ad Hoc Networks (Q1, IF=3.151)*, September 2018.

CONFERENCES

1. M. A. Vázquez-Castro, P. Saxena, **Tan Do-Duy**, T. Vamstad, and H. Skinnemoen, "SatNetCode: Functional design and experimental validation of network coding over satellite", in *the International Symposium on Networks, Computers and Communications (ISNCC)*, Rome, Italy, June 2018.

Chapter 5

Network Coding Functionality to Enhance Connectivity over Converged Satellite-Cloud Networks

In this chapter, we validate the performance of our proposed NCF design through a complete use case to enhance MANETs connectivity over converged satellite-cloud networks. Our motivation is illustrated in the system architecture shown in Figure 2.1 where MANETs are assisted by a satellite since an emergency situation disconnects MANETs from local terrestrial networks.

Device-to-device (D2D) is proposed as a promising 5G technology for direct communication between mobile devices. Under such scenario, we assume D2D technology to enhance MANETs for emergency applications. Due to highly unreliable MANET links, we tackle the problem of increasing the connectivity to enhance the MANET coverage (e.g. to relief teams) using per-flow NC. While NC can theoretically achieve capacity, encoding, re-encoding, and decoding functions may require high energy expenditure of MANET power-limited devices. Further, in an emergency scenario there may not be direct access to fog or cloud computing, which will then be provided via satellite. Hence, the only local computational resources available are the MANET devices. To solve this situation, we propose a centrally-controlled optimization of per-path finite-length coding rates to balance the computation required at the nodes measured in use of logic gates and connectivity over the path. In this chapter, we design a NCF balancing computational resources and resulting coverage taking into account packet delay constraints. We do so by first of all identifying inputs whose availability is guaranteed under 5G technology assumption. The output is the per-path optimal coding rate, which is identified based on a novel proposal of searching algorithms. We then analyze the

performance of our NCF by measuring the gain in achievable rate and connectivity over the path with packet loss rate under a certain threshold.

5.1 Contributions and Structure

5.1.1 Contributions of the Chapter

This chapter presents the contributions that meet Objective 4 of this thesis, as defined in Section 1.2:

- **Objective 4: Apply the NCF design developed in Objective 1 and validate its performance for a complete use case in 5G network scenarios.**
  - Towards the forth objective of this thesis, we consider a study case e.g., enhancing network connectivity of MANET devices over converged satellite-cloud networks in an emergency scenario where the communication scenario is part of the network model in the EU H2020 GEO-VISION project. First, we define a packet-level NCF with inputs from data service quality targets, local computation constraints and per-path statistics. Outputs are optimal coding rates balancing per-node computational resources and resulting coverage. Then, we formulate, solve and analyze the centrally-controlled optimization problem for typical values of computational resources at network nodes. Simulation results show that our solution enables line network connectivity for target number of nodes even for power-limited devices (e.g. smartphones). This is in contrast with connectivity not being feasible at all without our solution.

5.1.2 Structure of the Chapter

The rest of this chapter is structured as follows. In Section 5.2, we give an overview of the system model that we consider in this chapter. In Section 5.3, we describe the design of the NCF. In Section 5.4, we show the analysis of our NCF based on a comprehensive set of simulations. Finally, we identify some conclusions in Section 5.5.

5.2 System Model

The logical model of a set of MANETs, which are together centrally managed as those sketched in Figure 2.1 can be modeled as an acyclic graph $\mathcal{G}' = (\mathcal{V}', \mathcal{E}', \mathcal{D}')$ where $\mathcal{V}'$ and

$\mathcal{E}'$ are the set of logical associated nodes and directed links in the network, respectively. $\mathcal{D}'$ is the set of random variables corresponding to the erasure process associated with each communication link according to some order. We consider random packet erasure model where each link i is modelled as a memoryless channel erased with probability δ_i.

Even if the problem of routing can clearly be linked to the problem of enabling network coded reliable paths for network flows, we do not consider the routing problem. This is because we foresee a first stage of operation of converged cloud-satellite networks leveraging existing efficient routing protocols. In principle, multi-path transmission between the source and the destination could bring out many advantages for the network such as fault tolerance and higher throughput [60]. However, in MANETs, multi-path transmission may have many disadvantages if compared to single-path transmission. For instance, the complexity and overhead of route discovery in multi-path transmission is much more than that of the single-path case. Moreover, interference may cause significant degradation of quality of neighboring transmission using shared wireless channel [60]. Therefore, single-path routing protocols would be sufficient to enable efficient transmission of single flows between the network nodes. Consequently, we assume that efficient routing protocols are operating (see e.g. AODV, OSPF [14]). Hence, we consider that every optimized path between the source and the final destination is given to our NCF as a multihop line network $\mathcal{G} = (\mathcal{V}, \mathcal{E}, \mathcal{D}) \subset \mathcal{G}'$ where $\mathcal{V} \subset \mathcal{V}'$, $\mathcal{E} \subset \mathcal{E}'$, and $\mathcal{D} \subset \mathcal{D}'$ denote the corresponding set of logical nodes, directed links and the vector of per-link erasure rates in $\mathcal{G}$, respectively. We denote $\delta_i \in \mathcal{D}$ as the i-th link erasure rate, $1 \leq i \leq |\mathcal{E}|$. If all the erasure processes are equal, we use a unique value δ.

We assume that a packet stream is produced at the source node where the network traffic could be video or images. For Galois field of size $q = 2^m$, we use L symbols as the packet length including M symbols for information field and $L - M$ symbols for all header information.

In the following, we focus on a particular information flow as a sequence of transmitted packets along a line network $\mathcal{G}$ with $\mathcal{N}$ nodes and $\mathcal{L}$ links (path length). We note that any node in the path can also be receivers. We will be interested to compare the performance of our network coded flows with the case of routing. Some useful definitions are as follows:

Definition 2. ***Coding rate,*** ρ*, is the ratio between the number of information packets and the number of packets sent by the source node.*

Definition 3. ***Achievable rate at the*** n***-th node in*** $\mathcal{G}$ ***with NC,*** $R_{NC}^n(\mathcal{D}, \rho)$*, is defined as*

$$R_{NC}^n(\mathcal{D}, \rho) = \rho \left(1 - P_e^n(\mathcal{D}, \rho)\right)$$

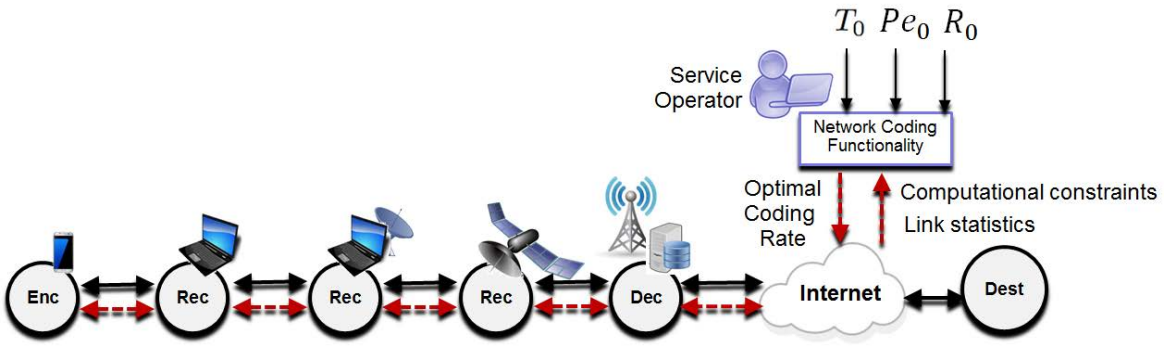

Fig. 5.1 Logical representation of a line network with $\mathcal{N} = 5$ nodes and $\mathcal{L} = 4$ links. The satellite is assumed to be regenerative with recoding functionalities. Black arrows represent information data flows and red arrows represent control data flow to assist MANET communication as designed by the service operator using the NCF.

with $P_e^n(\mathcal{D},\rho)$ the packet loss rate (PLR) at the n-th node with NC after decoding, $1 < n \leq \mathcal{N}$.

Definition 4. ***Achievable rate at the n-th node in $\mathcal{G}$ with routing,*** *$R_R^n(\mathcal{D})$, is defined as*

$$R_R^n(\mathcal{D}) = \prod_{i=1}^{n-1}(1-\delta_i)$$

with δ_i the per-link erasure rate.

Definition 5. ***Achievable rate gain at the n-th node in $\mathcal{G}$:*** *is defined as $\Delta R^n(\mathcal{D},\rho) = \frac{R_{NC}^n(\mathcal{D},\rho)-R_R^n(\mathcal{D})}{R_R^n(\mathcal{D})}$ (in %) for some coding rate ρ.*

Definition 6. ***Computational complexity:*** *the amount of computational resources needed for coding operations at the n-th node in $\mathcal{G}$ $(1 \leq n \leq \mathcal{N})$ denoted by $\beta^n(\mathcal{D},\rho)$. Constraint on computational resources of the n-th node and the vector of per-node computational resources is denoted by β_0^n and $\mathcal{B}$, respectively.*

5.3 Network Coding Functionality

In this section, we present our design of a packet-level NCF for the use case following the NC functional design in Chapter 3.

As justified above, our design is independent of routing policy and therefore every NCF instantiation is in one-to-one correspondence with an (aggregated or single) information flow. Hence, it is enough to focus on the design of a NCF for a line network $\mathcal{G}$ with $\mathcal{N}$ nodes and

$\mathcal{L}$ links. An example of logical representation of one such line network with $\mathcal{N} = 5$ nodes and $\mathcal{L} = 4$ links is showed in Figure 5.1. Black arrows represent information data flows and red arrows represent control data flow to assist MANET communication as designed by the service operator using the NCF. Note that when the satellite repeater is assumed to be regenerative, then it can run re-encoding functionalities. Given the definition of NCF proposed in Section 3.4, we provide the functional design of NCF as follows.

5.3.1 Inputs and Output

We assume our NCF has the following inputs from the MANETs:

- **Vector of per-link erasure rates,** $\mathcal{D}$. We assume per-link erasure rates are updated to the NCF periodically.
- **Vector of per-node computational resources,** $\mathcal{B}$. We assume this information can be pulled from the nodes to the NCF.

Computational resources at the nodes are considered as the total number of logic gates required for implementing multiplication and addition operations over $GF(2^m)$. We also assume the following inputs from the Service Operator:

- **Target achievable rate,** R_0. This is the quality target for the throughput of information flow set by the service operator.
- **Target PLR,** Pe_0. This is the quality target for the PLR of information flow set by the service operator.
- **In-order packet delay constraint,** T_0. We assume a network service (video or images) is produced at the source.

Given the above inputs, the NCF optimizes the achievable rate at a particular receiver in $\mathcal{G}$ while balancing the use of computational resources and the resulting coverage taking into account delay constraints. The output is the per-path optimal coding rate, which is signaled from the NCF to all nodes.

We then define connected nodes and connectivity over a line path $\mathcal{G}$ with NCF and with routing as follows.

Definition 7. ***Connected node.*** *A n-th node in $\mathcal{G}$ $(1 < n \leq \mathcal{N})$ is said to be connected to the source node if*

$$R^n_{NC}(\mathcal{D},\rho) \geq R_0 \qquad or \qquad R^n_R(\mathcal{D}) \geq R_0$$

$$s.t.\quad P^n_e(\mathcal{D},\rho) \leq Pe_0, \qquad\qquad s.t.\ \ 1-\textstyle\prod_{i=1}^{n}(1-\delta_i) \leq Pe_0,$$
$$\beta^v(\mathcal{D},\rho) \leq \beta^v_0, \forall v \in [1,n]$$
$$T^n_{NC}(\mathcal{D},\rho) \leq T_0,$$

where $T^n_{NC}(\mathcal{D},\rho)$ denotes average in-order packet delay at the n-th node.

We call $\lambda_{NC}(R_0,Pe_0)$ and $\lambda_R(R_0,Pe_0)$ the number of connected nodes in $\mathcal{G}$ w.r.t. NCF and routing, respectively. Then, we define connectivity over a line path $\mathcal{G}$ as follows.

Definition 8. ***Connectivity over a line path*** $\mathcal{G}$***:*** *is defined as $\gamma_{NC}(R_0,Pe_0) = \lambda_{NC}(R_0,Pe_0)/\mathcal{L}$ and $\gamma_R(R_0,Pe_0) = \lambda_R(R_0,Pe_0)/\mathcal{L}$ (in %) with NCF and routing, respectively.*

5.3.2 Network Coding Schemes for NCF

Our proposed NCF can operate with any NC scheme, which we assume roughly classified into two broad classes: structured and random NC schemes. The coding performance of representative structured and random network codes has been evaluated in Chapter 4. In this chapter, we assume random NC schemes to reduce average packet delay. However, our methodology is equally applicable for any other type of NC schemes.

We note that for different practical uses of NC, the different design constraints e.g., packet delay and/or computational resources, may require different coding block-length [61, 59]. We thus study the performance of our NCF design with different random codes with finite-length coding rate. Specifically, we consider random linear capacity-achieving schemes: non-systematic (RLNC) and systematic (SNC) and non-capacity achieving schemes: SNC with packet scheduling (SNC-S) or sliding window (SWNC). The model for the encoding, re-encoding, and decoding process of the different random NC schemes in matrix notation and corresponding PLRs have been presented in Chapter 4.

5.3.3 Average In-order Packet Delay

Recall we are considering multi-hop line paths of a MANET with $\mathcal{N}$ nodes and $\mathcal{L}$ links. We assume that each node transmits a packet in a timeslot with slot duration τ_s (miliseconds) which is the same for all timeslots used by all nodes. Each packet is incurred transmission delay along the links in line path $\mathcal{G}$ including D2D links and satellite links. We assume that

transmission delay along D2D links is negligible. Then, overall transmission delay is equal to the transmission delay along satellite links and is denoted by τ_p (miliseconds).

Due to the lack of analytical models, we use extensive simulations to evaluate the average in-order packet delay at the n-th node. Specifically, for a stream of $|\mathcal{S}|$ information packets, let τ_j (in timeslots) denote the difference between the time a packet $j \in \mathcal{S}$ is transmitted by the source and the time that it is delivered in-order at the destination. For the set $\mathcal{S}^* \subset \mathcal{S}$ packets delivered successfully, average in-order packet delay at the n-th node in $\mathcal{G}$ $(1 < n \leq \mathcal{N})$ is given as $\tau_{nc}^n(\mathcal{D},\rho) = \frac{\Sigma_{j=1}^{|\mathcal{S}^*|}\tau_j}{|\mathcal{S}^*|}$ (in timeslots).

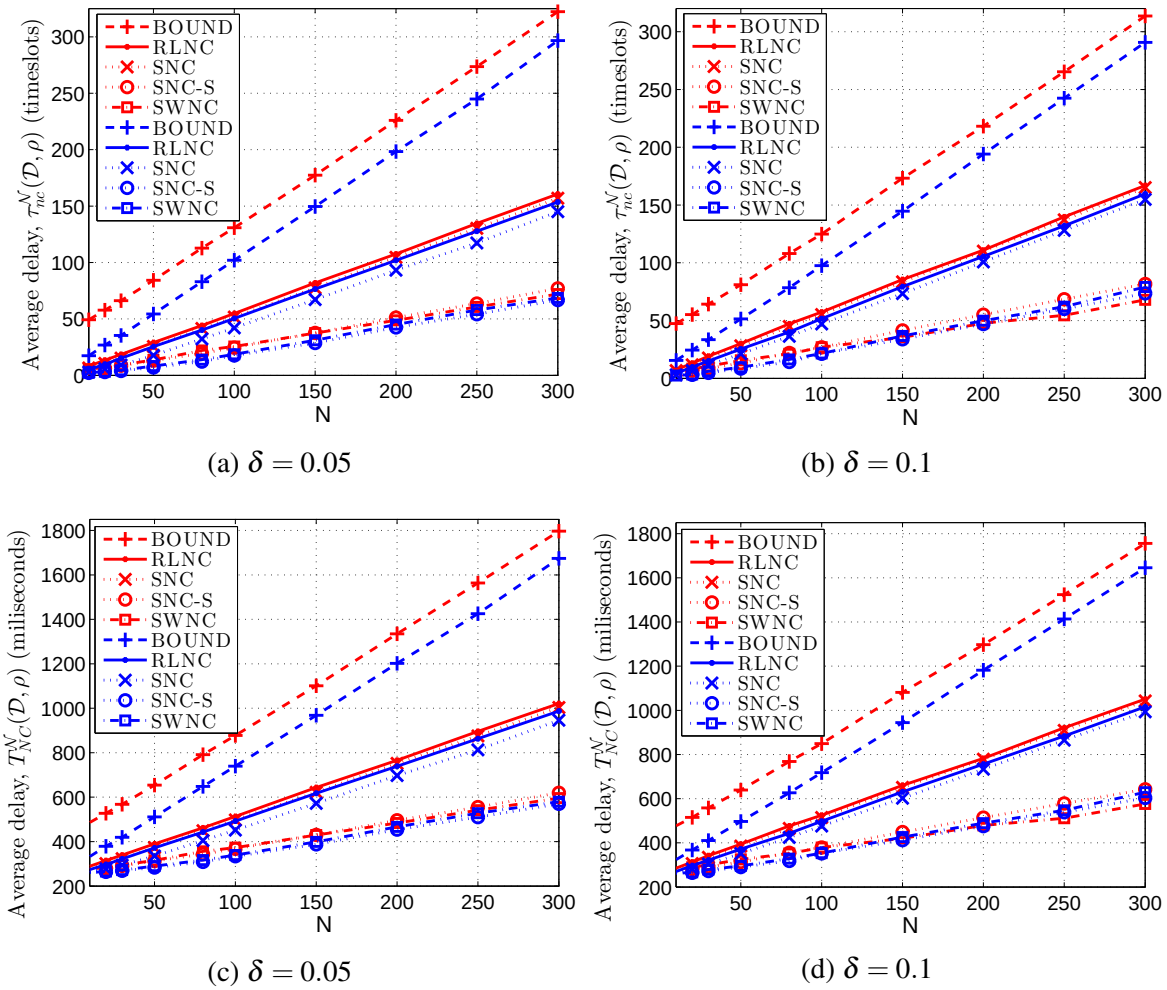

(a) $\delta = 0.05$ (b) $\delta = 0.1$

(c) $\delta = 0.05$ (d) $\delta = 0.1$

Fig. 5.2 Average in-order packet delay over 2-hop (blue) and 5-hop (red) line networks with $\delta = 0.05$ and $\delta = 0.1$ for a range of N with target $Pe_0 = 10^{-2}$ in timeslots (first row) and in miliseconds (second row).

For comparison, we use the packet delay bounds for random linear NC over line networks derived in [59] as a baseline packet delay model. We can infer that the average in-order

packet delay increases linearly with block-length N and path length $\mathcal{L}$ (a justification has been provided in Section 4.6.4). Finally, the average in-order packet delay (in miliseconds) at the n-th node in $\mathcal{G}$ is given as $T^n_{NC}(\mathcal{D},\rho) = \tau^n_{nc}(\mathcal{D},\rho)\tau_s + \tau_p$.

For illustration, in Figure 5.2, we show the average in-order packet delay for different NC schemes on 2-hop and 5-hop line networks with different erasure rates and block-length. We consider that the line network $\mathcal{G}$ includes $\mathcal{L}-2$ D2D links and two satellite links in order. We assume the flow bit-rate is 2.5 Mbps with packet length $L = 1500$ bytes ($q = 2^8$). Hence, the slot duration is $\tau_s = \frac{L*8}{2500} = 4.8$ ms and the transmission delay along satellite links is $\tau_p = 250$ ms [62]. The packet delay for different NC schemes is averaged over multiple simulations where coding rate is optimally identified by a searching algorithm e.g., Algorithm 1 in Chapter 4, that the target $Pe_0 = 10^{-2}$ representing delay-constrained applications [57] is satisfied. The figure also plots the bound of average packet delay with random linear NC to deliver the K information packets to the destination node in $\mathcal{G}$ [59]. The substantially low in-order packet delay with SNC-S is due to the fast loss determination and recovery of erased packets after the first half of each block. As for SWNC, notably low packet delay is because of short delay for recovering erased packets with the next coded packets [48].

5.3.4 Computational Complexity Model

We consider computational complexity in terms of the total number of logic gates required for implementing multiplication and addition operations over $GF(2^m)$ which can be approximated by m-bit arithmetic operations as $2m^2+2m$ and m logic gates, respectively [61]. We note that computational resources could be directly mapped to the energy consumption required at the nodes to perform coding operations, which largely depends on the specific platform and software implementation [61, 52].

Computational complexity for RLNC, SNC, SNC-S encoding in terms of logic gates can be obtained as

Proposition 3. *The computational complexity for RLNC/SNC/SNC-S encoding in terms of logic gates is*

$$\beta_{enc}(\rho) = N^M_{enc}(2m^2+2m) + N^A_{enc}m,$$

where $N^M_{enc} = \frac{K^2M}{\rho}$ *is the number of multiplications and* $N^A_{enc} = \frac{K(K-1)M}{\rho}$ *is the number of additions required for encoding process.*

Proof. We denote N packets generated by the encoder by matrix $X'_{1\times N} = X_{1\times K}G_{K\times N}$ where $X_{1\times K}$ is K information packets and $G_{K\times N}$ is the generator matrix in matrix notation. It is needed K multiplications and $K-1$ additions to generate a packet. Hence, for N packets,

we need NK multiplications and $N(K-1)$ additions. By applying the results in [61] with M symbols per packet and denoting N_{enc}^{M} and N_{enc}^{A} in terms of $\rho = \frac{K}{N}$, we obtain the equation of β_{enc}. □

Computational complexity of finite-length decoding based on Gauss-Jordan elimination algorithm is given as [63]:

Proposition 4. *The computational complexity for RLNC/SNC/SNC-S decoding in terms of logic gates can be obtained as* $\beta_{dec}^{n}(\mathcal{D},\rho) = N_{dec}^{M}(2m^2+2m) + N_{dec}^{A}m$,

$$\begin{aligned} N_{dec}^{M} &= \frac{\delta_{n-1}^{3}K^3}{3\rho^3} + \frac{\delta_{n-1}^{2}MK^2}{\rho^2} - \frac{\delta_{n-1}K}{3\rho}, \\ N_{dec}^{A} &= \frac{\delta_{n-1}^{3}K^3}{3\rho^3} + \frac{\delta_{n-1}^{2}\left(M-\frac{1}{2}\right)K^2}{\rho^2} + \frac{\delta_{n-1}\left(\frac{1}{6}-M\right)K}{\rho}, \end{aligned}$$

with δ_{n-1} *the erasure rate of packets received from the incoming link of the n-th node* $(1 < n \leq \mathcal{N})$.

As for SWNC, it has been showed in [48] that the computational complexity for encoding and for processing a sequence of $w_d = w_e$ consecutive packets in the decoder is equivalent to the computational complexity for the SNC/SNC-S encoder and decoder as showed in Proposition 3 and 4 with $K = w_e$ and $K = w_d$, respectively.

In general, computational resources required at a re-encoding node is upper bounded as

$$\beta_{rec}^{n}(\mathcal{D},\rho) \leq \beta_{dec}^{n}(\mathcal{D},\rho) + \beta_{enc}(\rho), \;\; 1 < n < \mathcal{N}.$$

Computational resources required at the source node and the destination node in $\mathcal{G}$ are given as $\beta^{1}(\rho) = \beta_{enc}(\rho)$ and $\beta^{\mathcal{N}}(\mathcal{D},\rho) = \beta_{dec}^{\mathcal{N}}(\mathcal{D},\rho)$, respectively.

From the above expressions we observe that, as expected, the lower the coding rate, the higher the required computational resources. Hence, computation-limited nodes will not be able to process NC schemes requiring low coding rates, which would be needed for bad channel conditions. We assume representative values for the available computational resources at the nodes e.g., $\beta_0^{phone} = 50 \times 10^6$, $\beta_0^{laptop} = 100 \times 10^6$, and $\beta_0^{server} = 500 \times 10^6$ logic gates, according to different platforms such as smartphones, laptops, and powerful computers or servers, respectively [52].

5.3.5 Network Coding Rate Optimization

The objective of the NCF is to identify the optimal coding rate ρ^* w.r.t. a particular receiver n in $\mathcal{G}$ $(1 < n \leq \mathcal{N})$ that maximizes the corresponding achievable rate, $R^n_{NC}(\mathcal{D}, \rho^*)$, while satisfying the target PLR, Pe_0, and the constraint of in-order packet delivery delay, T_0, given the vector of computational resources at the nodes, $\mathcal{B}$. Therefore, we define the following NC optimization problem that balances the number of nodes that attain the target PLR with optimized achievable rate and the required computational resources.

Proposition 5. ***NC optimization problem.*** *The optimal coding rate ρ^* is identified by the following optimization problem:*

$$\begin{aligned} & \rho^* = \underset{\rho}{argmax}\, R^n_{NC}(\mathcal{D}, \rho) \\ s.t.\quad & P^n_e(\mathcal{D}, \rho) \leq Pe_0, \\ & \beta^v(\mathcal{D}, \rho) \leq \beta^v_0, \\ & T^n_{NC}(\mathcal{D}, \rho) \leq T_0, \end{aligned} \tag{5.1}$$

with $1 < n \leq \mathcal{N}$, $\beta^v_0 \in \mathcal{B}$, $\forall v \in [1, n]$. The average in-order packet delay at the n-th node with a particular NC scheme, $T^n_{NC}(\mathcal{D}, \rho)$, is evaluated via simulations.

The identification of the optimal coding rate in Problem (5.1) can be facilitated by the following proposition.

Proposition 6. *A searching algorithm is sufficient to identify an optimal coding rate ρ^*_N w.r.t. a receiver n in $\mathcal{G}$ which is the largest coding rate given N such that all constraints in Problem (5.1) hold. Then, for a range of N, there exists a region of exponential optimal coding rate (ρ^*_N) increase.*

Proof. See Section 4.5. □

From Proposition 6, we observe that as $P^n_e(\mathcal{D}, \rho^*_N(N)) \approx Pe_0$, $R^n_{NC}(\mathcal{D}, \rho^*_N(N)) \approx \rho^*_N(N)\big(1 - Pe_0\big)$ given Pe_0. Hence, when $\rho^*_N(N)$ increases with N , $R^n_{NC}(\mathcal{D}, \rho^*_N(N))$ increases accordingly. Thus, the maximum achievable rate corresponds the largest $\rho^*_N(N)$ that all constraints in Problem (5.1) are satisfied for a range of N. Hence, $\rho^* = \max_N \rho^*_N(N)$.

Therefore, we propose Algorithms 2 and 3 based on our proposed Algorithm 1 (in Chapter 4) to identify ρ^* and the corresponding optimal achievable rate $R^n_{NC}(\mathcal{D}, \rho^*)$. Algorithm 2 identifies an optimal coding rate according to a specific N, ρ^*_N, and $R^n_{NC}(\mathcal{D}, \rho^*_N)$ given Pe_0 and the constraints of computational resources and average in-order packet delay while Algorithm 3, which covers Algorithm 2, identifies ρ^* and $R^n_{NC}(\mathcal{D}, \rho^*)$ for a given range of N. More specifically, in Algorithm 2, by assuming $K = \lceil N\rho \rceil$ (or $w_e = \lceil N\rho \rceil$ in SWNC) given

Algorithm 2 Identification of the optimal coding rate for a specific N, ρ_N^*, and $R_{NC}^n(\mathcal{D},\rho_N^*)$.

Initialize
  Set $\mathcal{L}$, $\mathcal{D}$, N, n, Pe_0, $K=\lceil N\rho\rceil$ (or $w_e=\lceil N\rho\rceil$)
  For a set Ψ_N of coding rate, $\rho[i]\in\Psi_N$, $1\le i\le|\Psi_N|$
  $first=1$, $last=|\Psi_N|$, $\rho_N^*=\emptyset$, $R_{NC}^n(\mathcal{D},\rho_N^*)=\emptyset$
while $(first<last)$ {
  $mid=\lfloor\frac{first+last}{2}\rfloor$
  Compute $P_e^n(\mathcal{D},\rho[mid])$, $\beta^n(\mathcal{D},\rho[mid])$, $T_{NC}^n(\mathcal{D},\rho[mid])$ (expressions or simulation)
  if $mid=first$
    if $P_e^n(\mathcal{D},\rho[mid])\le Pe_0$ & $\beta^n(\mathcal{D},\rho[mid])\le\beta_0^n$ & $T_{NC}^n(\mathcal{D},\rho[mid])\le T_0$
      $\rho_N^*=\rho[mid]$
      $R_{NC}^n(\mathcal{D},\rho_N^*)=R_{NC}^n(\mathcal{D},\rho[mid])$
    break
  else if $P_e^n(\mathcal{D},\rho[mid])\le Pe_0$
    $first=mid$
    if $\beta^n(\mathcal{D},\rho[mid])\le\beta_0^n$ & $T_{NC}^n(\mathcal{D},\rho[mid])\le T_0$
      $\rho_N^*=\rho[mid]$
      $R_{NC}^n(\mathcal{D},\rho_N^*)=R_{NC}^n(\mathcal{D},\rho[mid])$
  else
    if $\beta^n(\mathcal{D},\rho[mid])\le\beta_0^n$ & $T_{NC}^n(\mathcal{D},\rho[mid])\le T_0$
      $last=mid$
    else **break** }
Return ρ_N^* and $R_{NC}^n(\mathcal{D},\rho_N^*)$

Algorithm 3 Identification of the optimal coding rate for a range of N, ρ^*, and $R_{NC}^n(\mathcal{D},\rho^*)$.

Initialize
  Set $\mathcal{L}$, $\mathcal{D}$, n, Pe_0
  For a set Θ of N, $N[i]\in\Theta$, $1\le i\le|\Theta|$
  $first=1$, $last=|\Theta|$, $\rho^*=\emptyset$, $R_{NC}^n(\mathcal{D},\rho^*)=\emptyset$
while $(first<last)$ {
  $mid=\lfloor\frac{first+last}{2}\rfloor$
  Run Algorithm 2 $\big($input $N=N[mid]$, output ρ_N^* and $R_{NC}^n(\mathcal{D},\rho_N^*)\big)$
  if $mid=first$
    $\rho^*=\rho_N^*$
    $R_{NC}^n(\mathcal{D},\rho^*)=R_{NC}^n(\mathcal{D},\rho_N^*)$
    break
  else if $\rho_N^*\neq\emptyset$
    $first=mid$
    $\rho^*=\rho_N^*$
    $R_{NC}^n(\mathcal{D},\rho^*)=R_{NC}^n(\mathcal{D},\rho_N^*)$
  else $last=mid$ }
Return ρ^*, $R_{NC}^n(\mathcal{D},\rho^*)$

N, PLR for a specific NC scheme is considered as a function of ρ and $\mathcal{L}$. We denote Ψ_N as the set of coding rates available for searching with regard to a particular N. Moreover, we denote Θ as the set of N available for Algorithm 3 to identify ρ^*. Hence, in overall the complexity of Algorithm 3 is $\mathcal{O}(log_2|\Psi_N^m|log_2|\Theta|)$ with $|\Psi_N^m| = \max_{N\in\Theta}|\Psi_N|$ [55, 64].

5.4 Performance Evaluation

In this section, we provide simulation results in Matlab to evaluate the performance of our designed NCF according to different random NC schemes with regard to the impact of link statistics and design constraints. We show how the NCF could adapt itself at the optimal coding rate ρ^* to attain the optimal achievable rate gain and balance the connectivity over a line path $\mathcal{G}$ and required computational resources.

5.4.1 Simulation Settings

We consider an emergency scenario as showed in Section 5.2 where satellite is employed to support the connectivity between a source-destination pair. We assume that a single-path routing protocol is available so that NCF can be implemented at all nodes. Then, we evaluate the optimal achievable rate and connectivity over a line path $\mathcal{G}$. Coding rate is optimized according to the NC optimization problem proposed in Proposition 5, which is then solved by Algorithms 2 and 3. The block-length range is given according to the region of exponential optimal coding rate increase, $10 \leq N \leq 100$ (see Chapter 4).

We assume a path $\mathcal{G}$ with $\mathcal{N}$ nodes and $\mathcal{L}$ links as illustrated in Figure 5.1, including $(\mathcal{L}-2)$ D2D communication links and 2 satellite links in order. We assume low and high per-link erasure rates. Specifically, all D2D links undergo the same erasure rate e.g., $\delta_{D2D} = 0.05$ or 0.1 representing 802.11 wireless links [58]. We assume realistic GEO satellite transmission with links affected by light rainfall e.g., $\delta_{SAT} = 0.1$ or 0.2 [47, 65]. Packet length is $L = 1500$ bytes with information length $M = 1400$ bytes ($m = 8$, $q = 2^8$) with a flow bit-rate of 2.5 Mbps [66]. Transmission delay over satellite is $\tau_p = 250$ ms [62]. We consider two types of network traffic:

- For video, the target PLR is $Pe_0 = 10^{-2}$ representing delay-constrained applications while packet delay constraint over satellite is $T_0 = 1000$ ms [57, 62].
- For images, it is generally expected that there is zero errors and delay requirements are low e.g., $Pe_0 = 10^{-6}$ and $T_0 = 2000$ ms [62].

However, we note that the proposed algorithms can operate with any target PLR and erasure rate. In Fig. 5.3, we illustrate a line network with the values we consider in the simulations. For illustration, we also assume the same computational resource constraints for all nodes, $\beta_0^n = \beta_0$ $(\forall n \in [1,\mathcal{N}])$. Each node has either low, moderate, or high computational resources representing different platforms such as smartphones, laptops, and servers, respectively, as mentioned in Section 5.3.4.

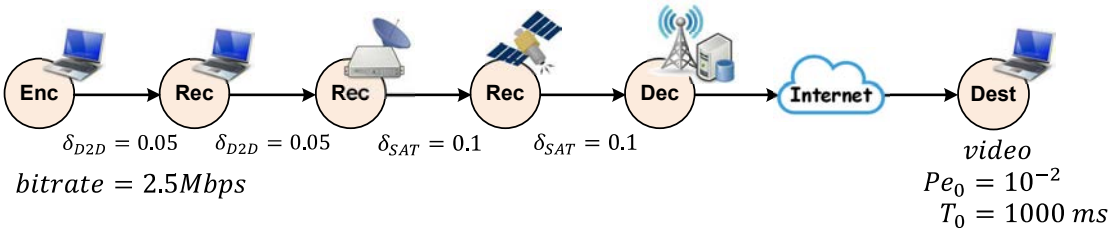

Fig. 5.3 An illustration of a line network with $\mathcal{N} = 5$ nodes and $\mathcal{L} = 4$ links with the settings we consider in the simulations for video traffic where the links are modeled as erasure channels with erasure rates $\delta_{D2D} = 0.05$ (D2D links) and $\delta_{SAT} = 0.1$ (satellite links).

5.4.2 Achievable Rate

Optimal Achievable Rate

In Figure 5.4, we show the optimal achievable rate with our NCF w.r.t. different NC schemes and with routing at the destination node in $\mathcal{G}$ as a function of path length $\mathcal{L}$ for different representative devices. We note that the capacity of the topology is the min-cut of the networks which is given by $\min_{1\leq i\leq \mathcal{L}} \left(1-\delta_i\right)$.

Major conclusions can be inferred as follows:

- For the same per-link erasure rates and representative devices, the longer the path length $\mathcal{L}$ i.e., the more the re-encoding times, the lower the optimal achievable rate. This is because as observed from Eq. (4.6) (in Section 4.5), for any ρ, $P_e^{\mathcal{N}}(.)$ is an increasing function of $\mathcal{L}$. Thus, the higher the $\mathcal{L}$, the lower the optimal coding rate is needed [23].

- Without NCF, achievable rate with routing dramatically decreases and could reach to zero when $\mathcal{L}$ is sufficiently large. Also importantly, routing might not guarantee low target PLR for video services [57, 62] at any node beyond the source node.

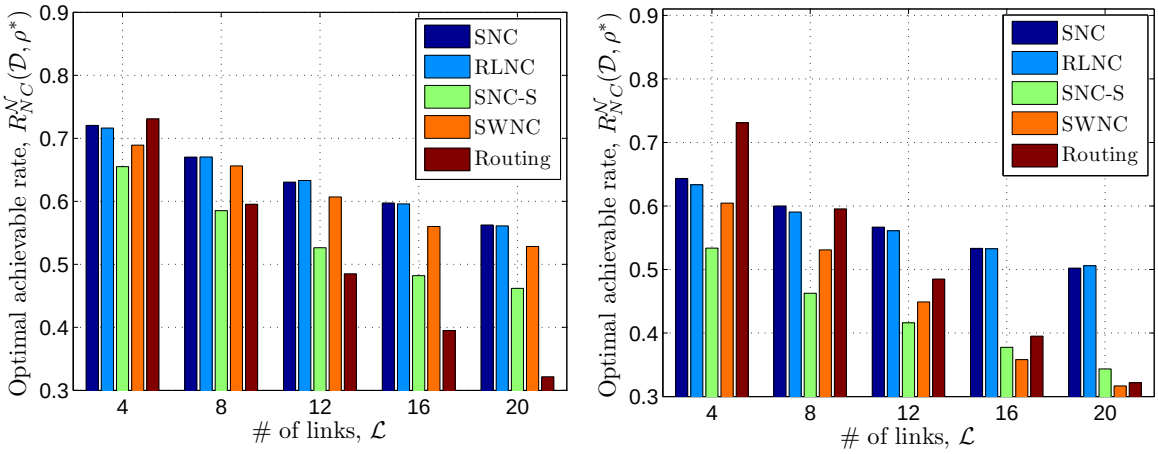

(a) Video

(b) Images

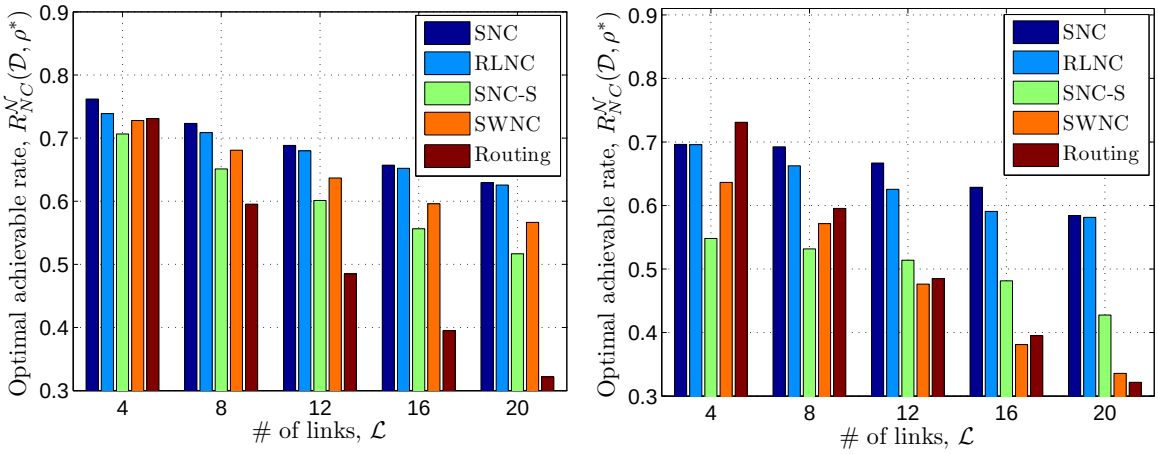

(c) Video

(d) Images

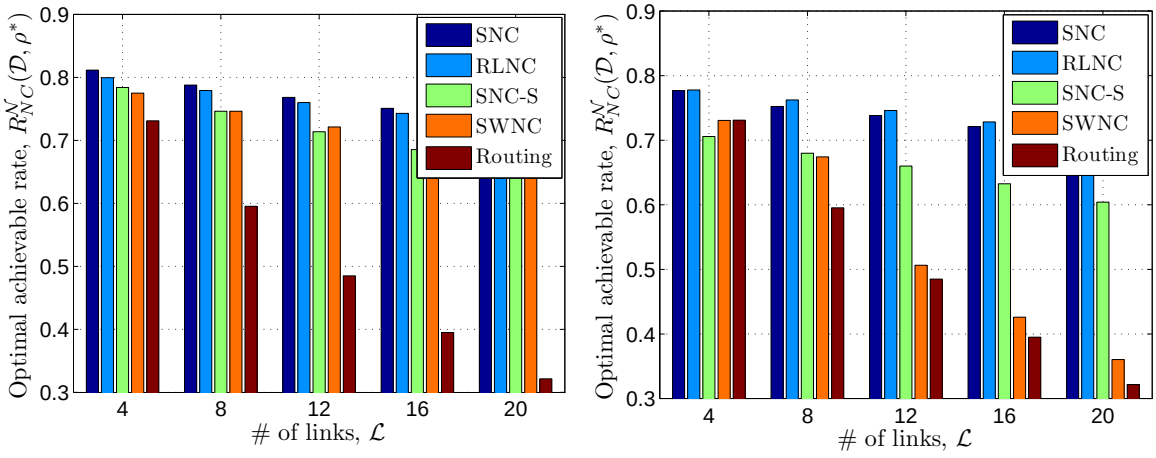

(e) Video

(f) Images

Fig. 5.4 Optimal achievable rate with our designed NCF according to different NC schemes and achievable rate with routing at the destination in $\mathcal{G}$, $R_{NC}^{\mathcal{N}}(\mathcal{D},\rho^*)$ and $R_{R}^{\mathcal{N}}(\mathcal{D})$, respectively, versus path length $\mathcal{L}$ for video and images with representative devices: smartphones (first row), laptops (second row), servers (third row), erasure rates $\{\delta_{D2D}=0.05,\delta_{SAT}=0.1\}$.

- For the same network service, the higher the available computational resources, the higher the optimal achievable rate due to the higher optimal coding rate. This indicates the impact of available computational resources at nodes in $\mathcal{G}$ on the performance of NCF. The reason is that since the optimal coding rate increases with N, K increases accordingly. Consequently, as showed in Propositions 3 and 4, the higher the K, the higher the computational resources required for the implementation of NC.
- For the same type of representative devices, the optimal achievable rate for the case of video is higher than that of the case of images since the latter requires strictly low PLR.
- Figure 5.4 also shows the intrinsic tradeoff between achievable rate and packet delay since capacity-achieving schemes (RLNC and SNC) present highest achievable rate, which decreases with packet scheduling techniques (SNC-S and SWNC) to reduce packet delay.

Achievable Rate Gain

From the results showed in Figure 5.4, Figure 5.5 plots the optimal achievable rate gain at the destination in $\mathcal{G}$ with SNC for NCF compared to routing. As expected, the achievable rate gain increases with number of links, available computational resources, and erasure rates. Further, for video, we can obtain higher achievable rate gain than that of the case of images. For instance, with smartphones, the achievable rate gain could reach approximately 80% and 300% for video and 60% and 240% for images at $\mathcal{L} = 20$ links according to $\{\delta_{D2D} = 0.05, \delta_{SAT} = 0.1\}$ and $\{\delta_{D2D} = 0.1, \delta_{SAT} = 0.2\}$, respectively. Moreover, as observed from Figure 5.4, the significant increase of the achievable rate gain with $\mathcal{L}$ is because of the higher slope of the (decreasing) achievable rate with routing compared to that of NCF.

Optimal versus Non-optimal Achievable Rate

The main target of the designed NCF is to identify the optimal coding rate that maximizes the achievable rate at the receiver in $\mathcal{G}$ while satisfying the design constraints. However, it can also work in a non-optimal mode where the NCF could involve a heuristic algorithm that utilizes the end-to-end PLR from the receiver feedback to choose a coding rate e.g. [67, 68]. Specifically, given a specific block-length N the heuristic algorithm would adjust adaptively the coding rate until all design constraints in Problem (5.1) are satisfied. Yet, the design of such a heuristic algorithm is beyond the scope of this thesis.

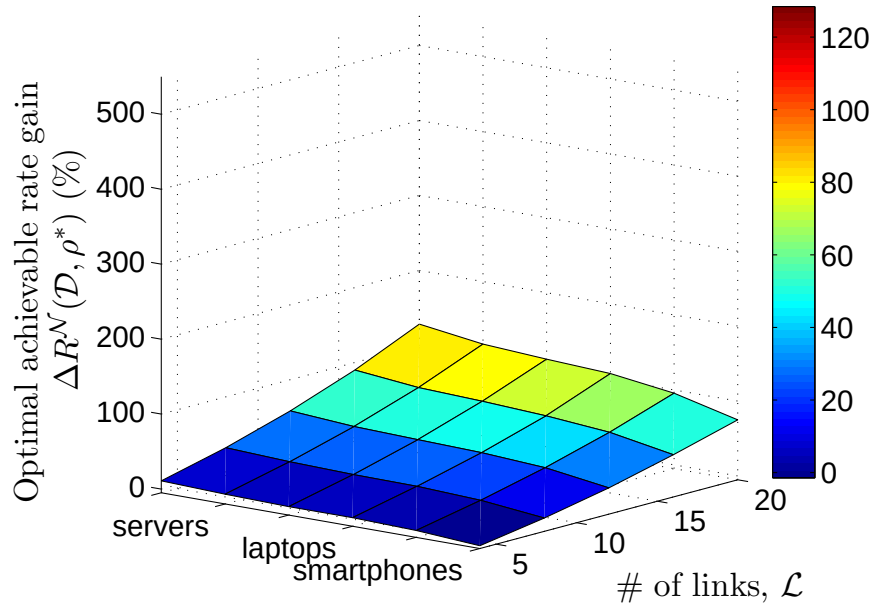

(a) $\{\delta_{D2D} = 0.05, \delta_{SAT} = 0.1\}$

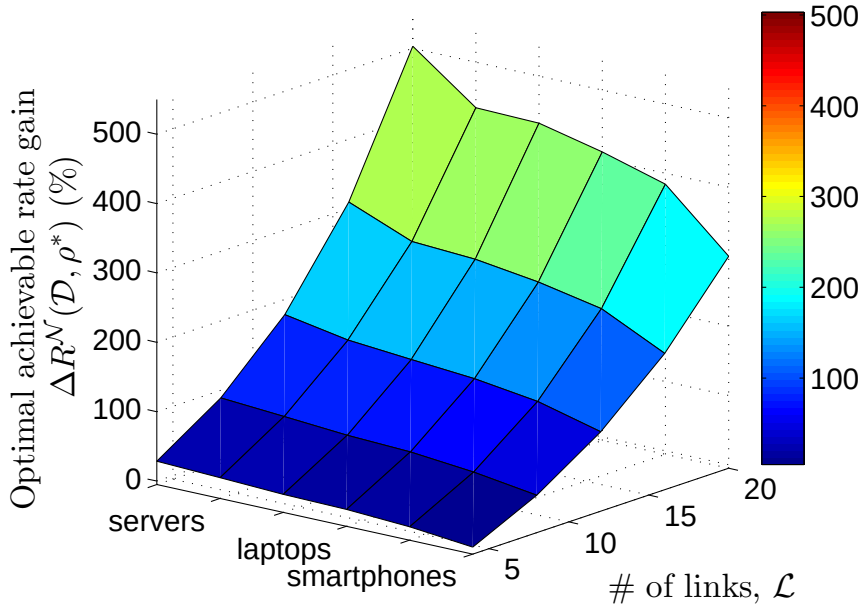

(b) $\{\delta_{D2D} = 0.1, \delta_{SAT} = 0.2\}$

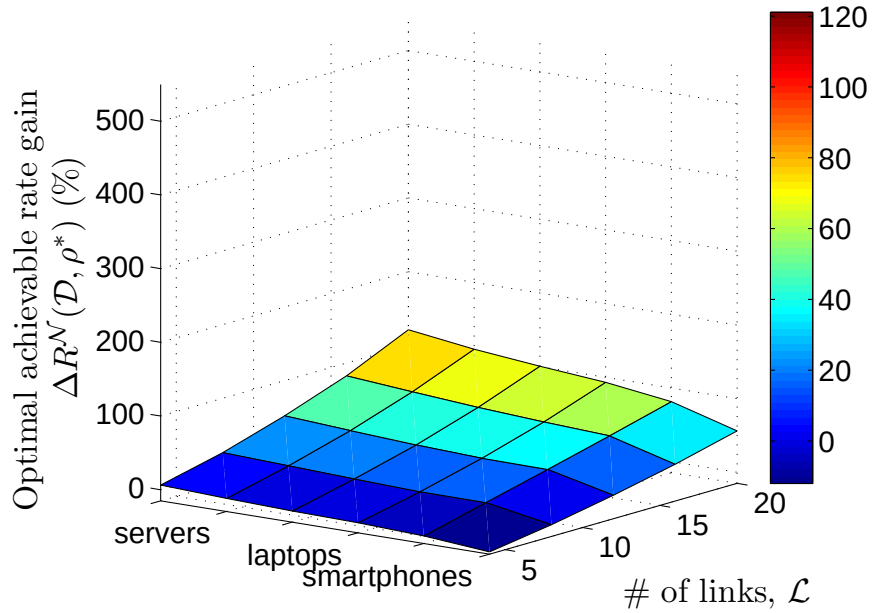

(c) $\{\delta_{D2D} = 0.05, \delta_{SAT} = 0.1\}$

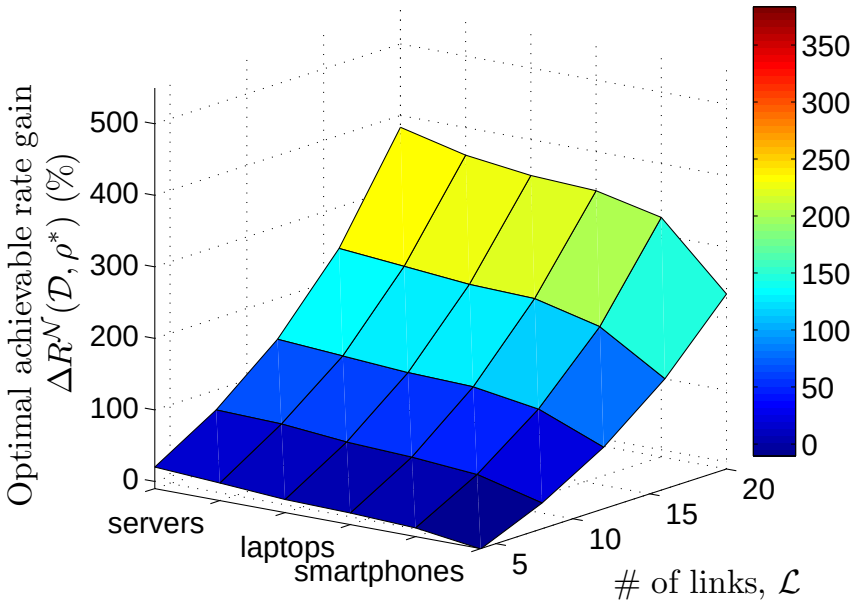

(d) $\{\delta_{D2D} = 0.1, \delta_{SAT} = 0.2\}$

Fig. 5.5 Optimal achievable rate gain compared to routing at the destination node in $\mathcal{G}$ with SNC for NCF, $\Delta R^{\mathcal{N}}(\mathcal{D},\rho^*)$ (in %), versus path length $\mathcal{L}$ with different representative devices and erasure rates, for illustrative traffic: VIDEO (Figs. 5.5a-5.5b) and IMAGES (Figs. 5.5c-5.5d).

We define achievable rate gain at the n-th node in $\mathcal{G}$ in response to the use of NCF with and without optimization as

$$\psi R^n(\mathcal{D},\rho^*) = \frac{R^n_{NC}(\mathcal{D},\rho^*) - R^n_{NC}(\mathcal{D},\rho^{'})}{R^n_{NC}(\mathcal{D},\rho^{'})}\ (in\%)$$

with ρ^* and $\rho^{'}$ the coding rate obtained from Problem (5.1) and from a heuristic algorithm e.g. [67], respectively.

In Figure 5.6, we show the achievable rate gain $\psi R^{\mathcal{N}}(\mathcal{D},\rho^*)$ at the destination node in $\mathcal{G}$. For the non-optimal mode, a fixed block-length is given e.g. $N = 30$ while for the optimization mode, the range of block-length is $10 \leq N \leq 100$. Figure 5.6 shows that NCF with optimization outperforms that of the non-optimal case. The higher the available computational resources and path length, the higher the achievable rate gain. This is because our proposed optimization algorithms can identify the optimal coding rate w.r.t. the maximum N depending on computational resources. The higher the available computational resources, the higher the N, and thus the higher the optimal coding rate.

5.4.3 Connectivity over a line path

We now evaluate how the computational resources at the nodes would impact the connectivity over a line path $\mathcal{G}$ when NCF is used. It is noted that with low target PLR for video and images [57], without NCF the connectivity over the path $\mathcal{G}$ could be zero with routing.

The results in Section 5.4.2 reveal that when a node n-th in $\mathcal{G}$ $(1 < n \leq \mathcal{N})$ is connected to the source node given target R_0, all intermediate nodes between the source and the n-th node are also connected. Hence, the connectivity over a particular $\mathcal{G}$ with $\mathcal{L}$ links is the ratio of $n_{max} - 1$ and $\mathcal{L}$, with $n_{max} - 1$ the maximum number of hops beyond the source node where the corresponding receiver, the n_{max}-th node $(1 < n_{max} \leq \mathcal{N})$, is still connected with coding rate optimized according to the n_{max}-th node.

In Figures 5.7 and 5.8, we show the connectivity over path $\mathcal{G}$ obtained with the use of NCF according to SNC with different target achievable rates e.g., $R_0 = 0.5, 0.6, 0.7$ [57], for video and images as illustrative traffic, respectively. The figures indicate that

- For the same $\mathcal{D}$ and representative devices, the connectivity reduces with path length $\mathcal{L}$ due to the decreasing achievable rate with number of links (see Figure 5.4).
- The connectivity over $\mathcal{G}$ goes down when the target R_0, erasure rate, and/or Pe_0 changes from low to high.

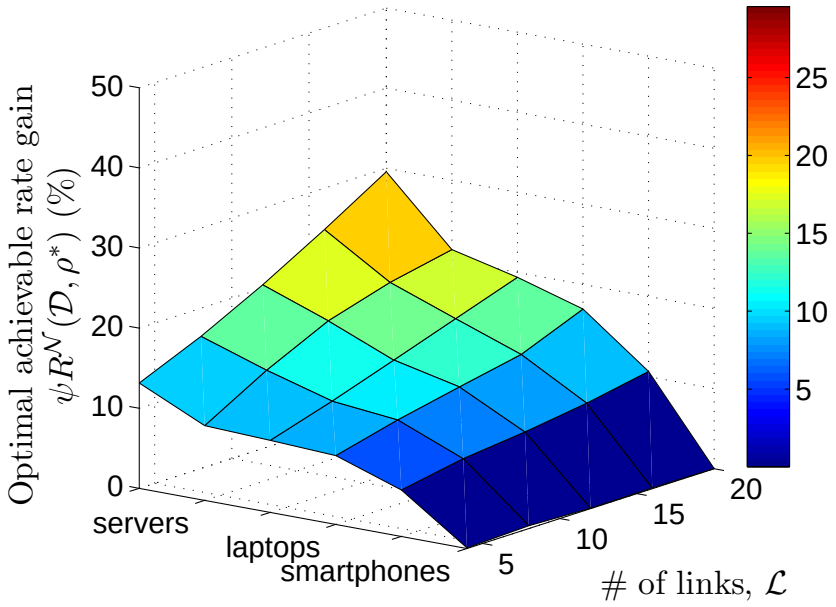

(a) $\{\delta_{D2D} = 0.05, \delta_{SAT} = 0.1\}$

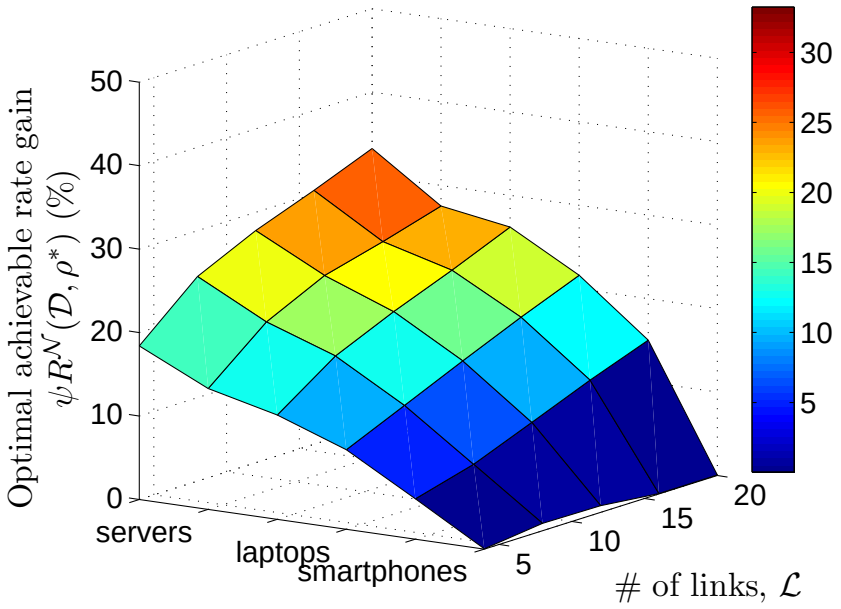

(b) $\{\delta_{D2D} = 0.1, \delta_{SAT} = 0.2\}$

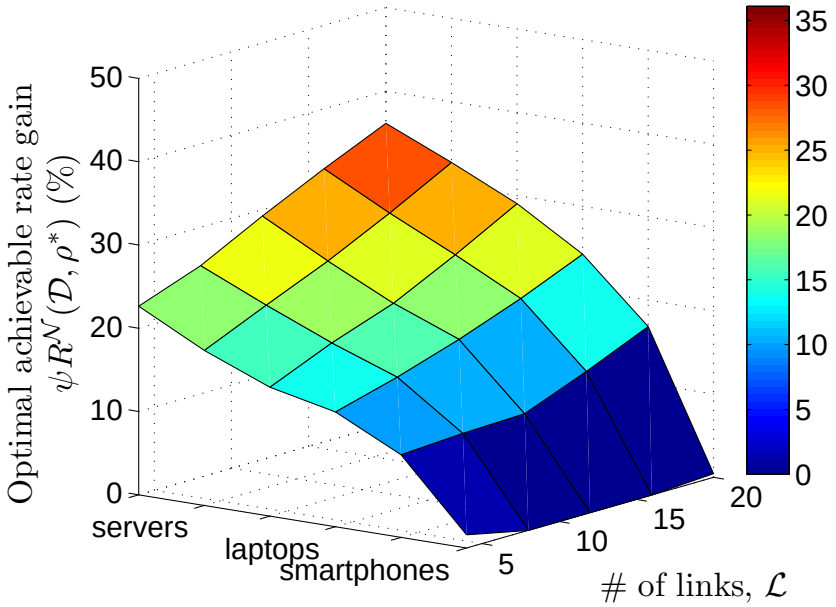

(c) $\{\delta_{D2D} = 0.05, \delta_{SAT} = 0.1\}$

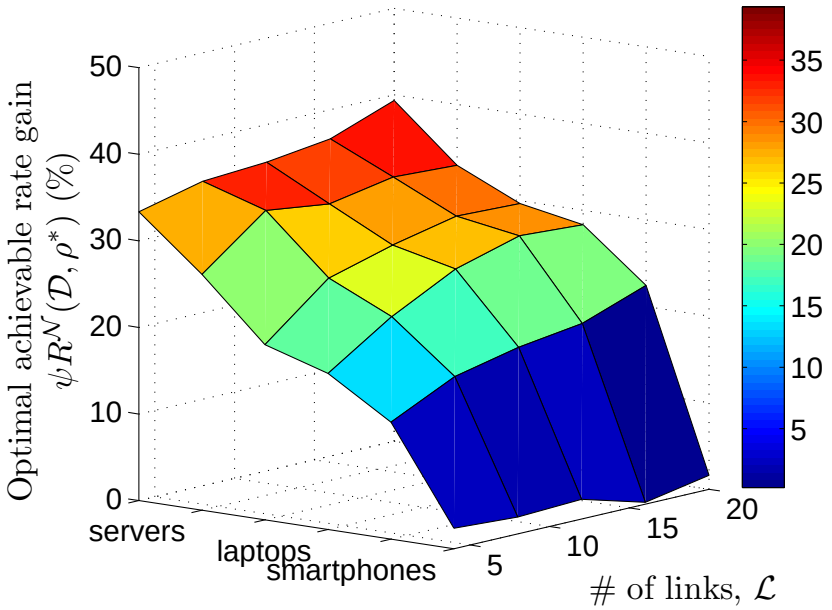

(d) $\{\delta_{D2D} = 0.1, \delta_{SAT} = 0.2\}$

Fig. 5.6 Achievable rate gain at the destination node in $\mathcal{G}$ according to the use of NCF w.r.t. SNC with optimal and non-optimal coding rate, $\psi R^{\mathcal{N}}(\mathcal{D},\rho^*)$ (in %), versus path length $\mathcal{L}$ with different representative devices and erasure rates, for illustrative traffic: VIDEO (Figs. 5.6a-5.6b) and IMAGES (Figs. 5.6c-5.6d).

- For the same per-link erasure rates and number of links, the higher the computational resources, the higher the connectivity over the path. Further, the connectivity with video is higher than that of images due to the higher achievable rate for the case of video. For instance, for $R_0 = 0.5$ with $\mathcal{L} = 20$ links and $\{\delta_{D2D} = 0.1, \delta_{SAT} = 0.2\}$, with video, the connectivity over the path $\mathcal{G}$ could reach up to some 75% and 90% with smartphones and laptops (Figure 5.7c), respectively, while with images the connectivity could only obtain approximately 50% and 80% with smartphones and laptops (Figure 5.8c), respectively.

- The figures show the tradeoff between the connectivity over a line network $\mathcal{G}$ with the use of NCF and the available computational resources which could be further mapped as energy cost of the nodes [61].

5.5 Conclusions

In this chapter, we have presented a NCF design to tackle the problem of enhancing the MANETs coverage for emergency scenarios. The NCF takes as inputs the service quality targets, the per-node computational resource constraints, and per-link per path erasure statistics. The function outputs the per-path optimal finite-length coding rates balancing computational resources required at the nodes and resulting connectivity. Simulation results show that the proposed NCF obtains significant gains in achievable rate and connectivity over the line path with different values of computational resources representing various types of commercial platforms.

Finally, the work in this chapter leads to the following publications.

JOURNALS

1. **Tan Do-Duy** and M. A. Vázquez-Castro, "Network Coding Function for Converged Satellite-Cloud Networks", *under review in IEEE Transactions on Aerospace and Electronic Systems (Q1, IF=2.063)*, August 2018.

CONFERENCES

1. **Tan Do-Duy** and M. A. Vázquez-Castro, "Geo-Network Coding Function Virtualization for Reliable Communication over Satellite", in *Proc. IEEE International Conference on Communications (ICC)*, Paris, France, May 2017.

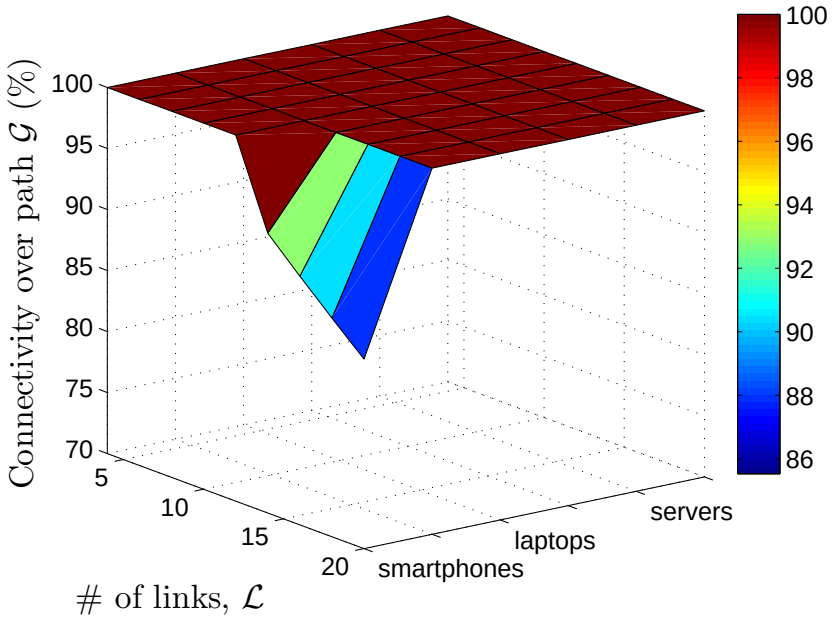
Connectivity over path $\mathcal{G}$ (%)
100
95
90
85
80
75
70
5
10
15
20
# of links, $\mathcal{L}$
smartphones
laptops
servers
100
98
96
94
92
90
88
86

(a) $R_0 = 0.6$

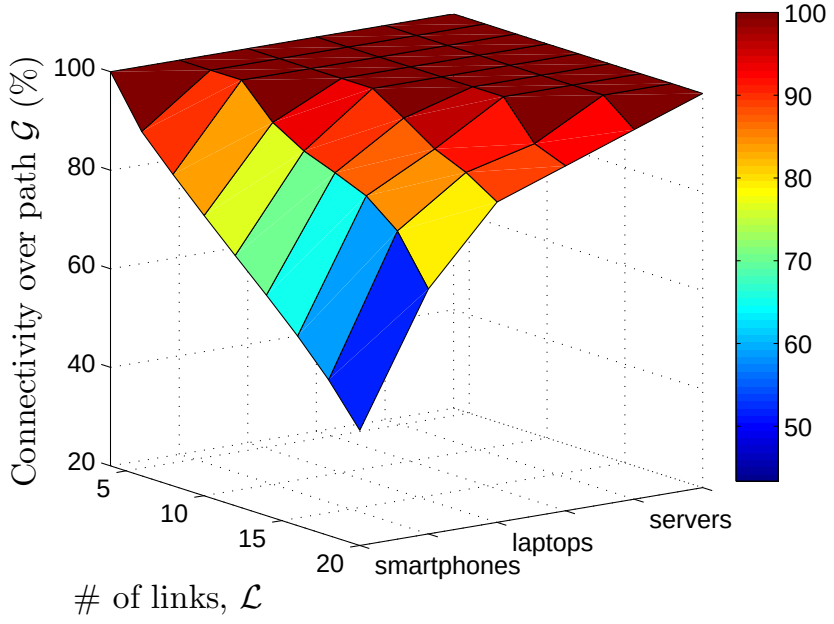
Connectivity over path $\mathcal{G}$ (%)
100
80
60
40
20
5
10
15
20
# of links, $\mathcal{L}$
smartphones
laptops
servers
100
90
80
70
60
50

(b) $R_0 = 0.7$

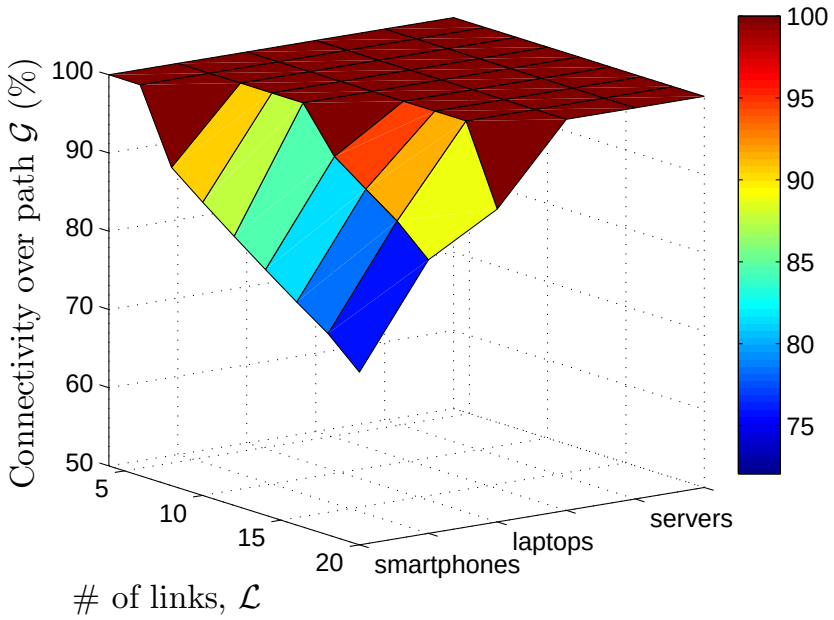

(c) $R_0 = 0.5$

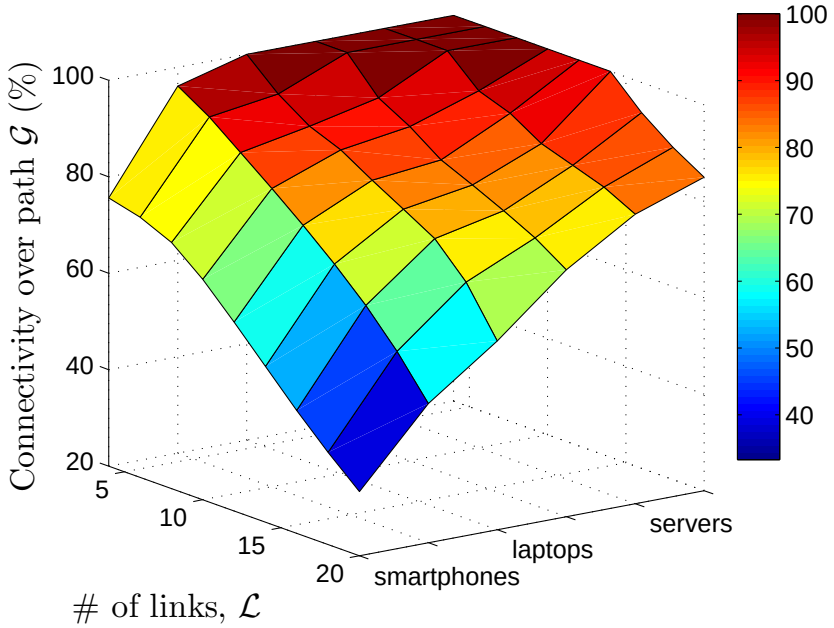

(d) $R_0 = 0.6$

Fig. 5.7 Connectivity over path $\mathcal{G}$ (%) obtained with the use of NCF according to SNC as a function of $\mathcal{L}$ with different representative devices for VIDEO with $\{\delta_{D2D} = 0.05, \delta_{SAT} = 0.1\}$ (Figs. 5.7a-5.7b) and $\{\delta_{D2D} = 0.1, \delta_{SAT} = 0.2\}$ (Figs. 5.7c-5.7d).

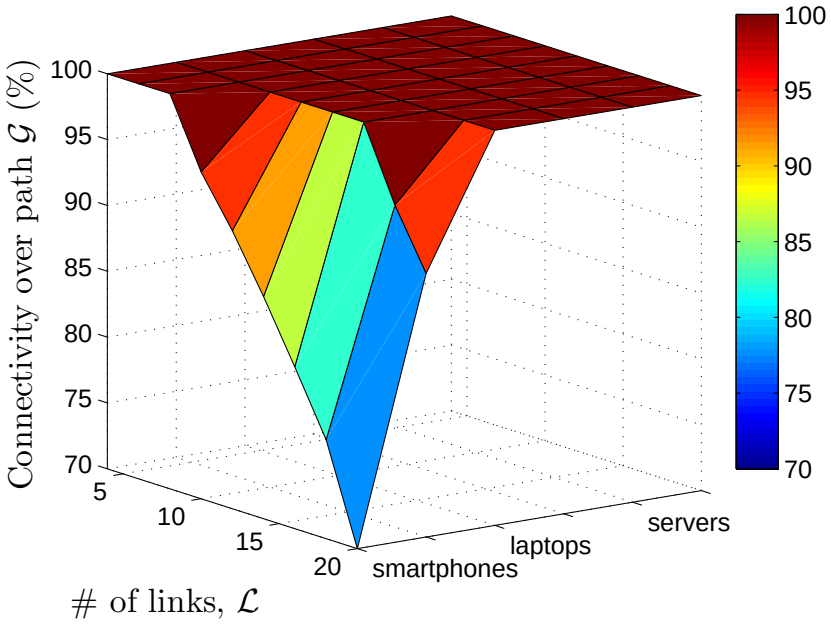
Connectivity over path $\mathcal{G}$ (%)
100
95
90
85
80
75
70
5
10
15
20
# of links, $\mathcal{L}$
smartphones
laptops
servers
100
95
90
85
80
75
70

(a) $R_0 = 0.6$

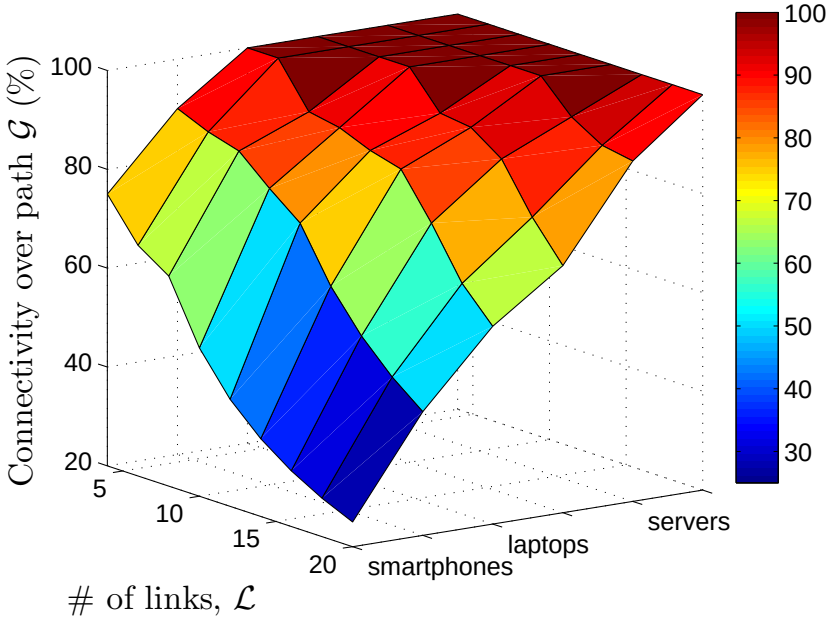
Connectivity over path $\mathcal{G}$ (%)
100
80
60
40
20
5
10
15
20
# of links, $\mathcal{L}$
smartphones
laptops
servers
100
90
80
70
60
50
40
30

(b) $R_0 = 0.7$

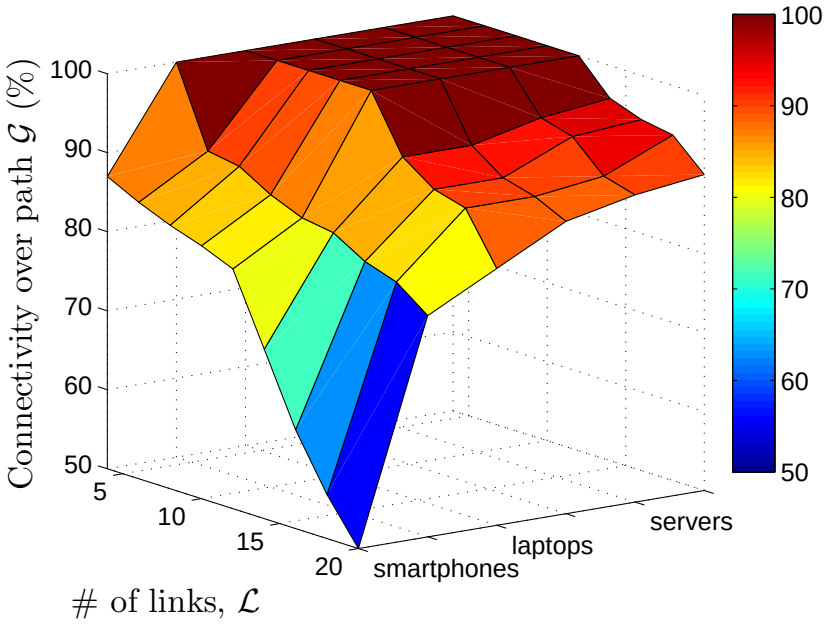

(c) $R_0 = 0.5$

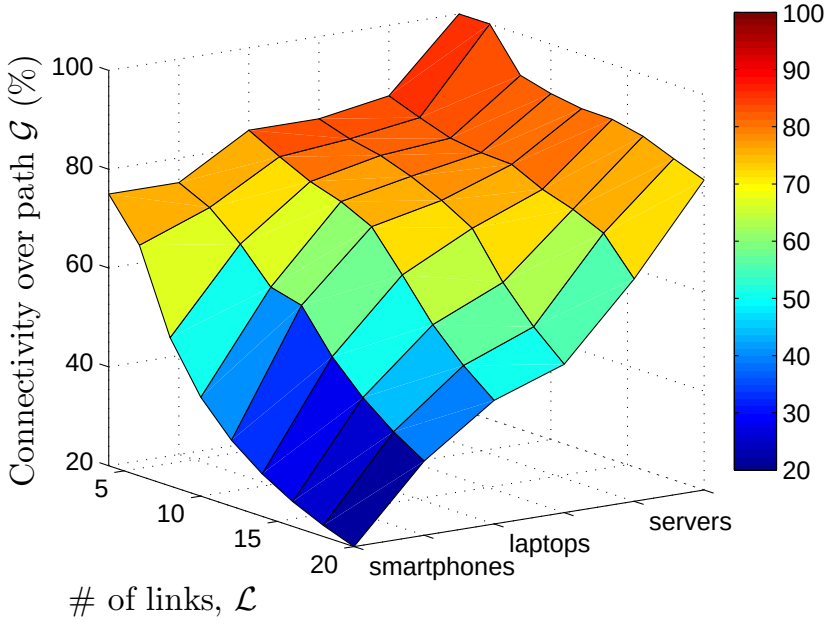

(d) $R_0 = 0.6$

Fig. 5.8 Connectivity over path $\mathcal{G}$ (%) obtained with the use of NCF according to SNC as a function of $\mathcal{L}$ with different representative devices for IMAGES with $\{\delta_{D2D} = 0.05, \delta_{SAT} = 0.1\}$ (Figs. 5.8a-5.8b) and $\{\delta_{D2D} = 0.1, \delta_{SAT} = 0.2\}$ (Figs. 5.8c-5.8d).

2. **Tan Do-Duy** and M. A. Vázquez-Castro, "Efficient Communication over Cellular Networks with Network Coding in Emergency Scenarios", in *2015 2nd International Conference on Information and Communication Technologies for Disaster Management (ICT-DM)*, Rennes, France, 2015, pp. 71–78.

Contributions to Project Deliverable Reports: EU H2020 GEO-VISION Project (2015-2017)

1. D2: 2.2 Technical Requirements and 2.3 System Design.

2. D3: 3.1 Research Technology, 3.2 Technology Development, and 3.3 Technology Integration Report.

Chapter 6

Overall Conclusions and Future Lines of Research

In this chapter, we conclude the thesis by summarizing our main contributions and presenting the future lines of research related to the contributions of this thesis.

6.1 Overall Conclusions

In this thesis, we studied the design and performance evaluation of a packet-level NCF working as a NF to facilitate the control of network throughput and reliability over 5G wireless networks. Based on the work done to achieve the main objectives, the overall conclusions of this thesis are summarized as follows:

- First, we developed a NC architectural design that could work as a traditional NF or be easily integrated in current proposals of virtualized network architectures. A toolbox of NC design domains has been identified so that NC can be designed as a NF that provides flow engineering functionalities to the network.
- Second, we presented a generic matricial model that allows us to analyze the corresponding error probabilities of different network codes over multi-hop line networks. The models can be used to analyze the performance of different packet-level NC schemes over line networks.
- Third, we proposed a methodology to characterize the finite-length coding performance in terms of achievable rate, average in-order packet delay, and coding overhead for different NC schemes which could be selected as the operational NC scheme for the proposed NCF with several design requirements. The performance evaluation

is done using both theoretical analysis and simulation results. Extensive simulation results show the throughput/delay trade-off between capacity-achieving vs non-capacity achieving random linear NC schemes and between capacity-achieving random linear NC schemes and structured codes using Pascal matrix with scheduling in the finite-length regime. The analysis done in this part provides a guide to the network designer in order to identify the best choice of practical codes and optimal coding rates depending on the user-case.

- Finally, we validated the performance of the proposed NCF design by working out a complete use case in 5G networks for controlled achievable rate and connectivity of MANET devices over converged satellite-cloud networks in emergency applications. Our results showed that with the proposed solution, line network connectivity can be guaranteed for target number of nodes even for power-limited devices e.g., smartphones, while in starkly contrast, the connectivity is not feasible at all without our solution. We also showed how this implies gains of orders of magnitude with respect to currently used routing mechanisms with PLR and delay below some thresholds according to video and images as illustrative traffic.

6.2 Future Lines of Research

We believe that the main contributions of our work can be extended to further work that allows to fully exploit the NC benefits in practical applications. This subsection presents the list of future directions to be considered in relation to the contributions of this thesis.

- **Extension to more complex network topologies:** this thesis only focuses on a line topology, a simple but common in practice network model. Yet, the analysis could be further extended to more complex network topologies such as a single-source multicasting/broadcasting or multi-source multi-destination network model. Modeling and evaluating the finite-length performance of different network codes in all these network models would provide the network designers with a guide to identify the optimal choice of network codes in order to attain a better performance of current communication networks.

- **Our proposed NCF can be tailored for different designs and accommodate additional functionalities:** this thesis focuses on a specific use case of our proposed NCF to enhance MANETs connectivity over converged satellite-cloud networks. However, the NC functional design and the NC optimization functionality can be adjusted

according to different use cases over wired and/or wireless networks (e.g., point-to-point/point-to-multipoint networks, heterogeneous networks, etc) with various service operational intents and network resources (e.g., computational resources, energy). Further, our NCF design can be used with packets at any higher layer in the OSI model.

- **Practical implementation of NCF:** the work in this thesis only investigates the functional design and performance validation of NCF through a complete use case. However, the NCF design can be implemented as a traditional NF or be easily integrated into the existing virtualized network architectures, leading to practical implementation and deployment in 5G networked systems.

References

[1] The European Telecommunications Standards Institute, "Network functions virtualisation (NFV); architectural framework," in *GS NFV 002 (V1.1.1)*, Oct. 2013.

[2] K. Chi, L. Huang, Y. Li, Y. h. Zhu, X. z. Tian, and M. Xia, "Efficient and reliable multicast using device-to-device communication and network coding for a 5g network," *IEEE Network*, vol. 31, no. 4, pp. 78–84, 2017.

[3] J. Hansen, D. Lucani, J. Krigslund, M. Medard, and F. Fitzek, "Network coded software defined networking: enabling 5G transmission and storage networks," *Communications Magazine, IEEE*, vol. 53, no. 9, pp. 100–107, 2015.

[4] J. Li, Y. Liu, Z. Zhang, J. Ren, and N. Zhao, "Towards green iot networking: Performance optimization of network coding based communication and reliable storage," *IEEE Access*, vol. 5, pp. 8780–8791, 2017.

[5] J. Huang, H. Gharavi, H. Yan, and C. C. Xing, "Network coding in relay-based device-to-device communications," *IEEE Network*, vol. 31, no. 4, pp. 102–107, 2017.

[6] D. Szabo, F. Nemeth, B. Sonkoly, A. Gulyas, and F. H. Fitzek, "Towards the 5G revolution: A software defined network architecture exploiting network coding as a service," *SIGCOMM Comput. Commun. Rev.*, vol. 45, pp. 105–106, 2015.

[7] L. F. Vieira and M. A. Vieira, "Network coding for 5g network and d2d communication," in *Proceedings of the 13th ACM Symposium on QoS and Security for Wireless and Mobile Networks*, ser. Q2SWinet '17, 2017, pp. 113–120.

[8] R. Ahlswede, N. Cai, S. Y. R. Li, and R. W. Yeung, "Network information flow," *IEEE Transactions on Information Theory*, vol. 46, no. 4, pp. 1204–1216, 2000.

[9] A. F. Dana, R. Gowaikar, R. Palanki, B. Hassibi, and M. Effros, "Capacity of wireless erasure networks," *IEEE Transactions on Information Theory*, vol. 52, no. 3, pp. 789–804, Mar. 2006.

[10] GEOVISION, *GNSS driven EO and Verifiable Image and Sensor Integration for mission-critical Operational Networks*. EU H2020 Projects, https://www.gsa.europa.eu/gnss-driven-eo-and-verifiable-image-and-sensor-integration-mission-critical-operational-networks.

[11] D. Kreutz, F. M. V. Ramos, P. E. Verissimo, C. E. Rothenberg, S. Azodolmolky, and S. Uhlig, "Software-defined networking: A comprehensive survey," *Proceedings of the IEEE*, vol. 103, no. 1, pp. 14–76, 2015.

[12] R. Mijumbi, J. Serrat, J. L. Gorricho, N. Bouten, F. D. Turck, and R. Boutaba, "Network function virtualization: State-of-the-art and research challenges," *IEEE Communications Surveys Tutorials*, vol. 18, no. 1, pp. 236–262, 2016.

[13] E. D. Re, S. Jayousi, S. Morosi, L. S. Ronga, M. D. Sanctis, E. Cianca, M. Ruggieri, E. Falletti, A. Iera, G. Araniti, and C. Sacchi, "SALICE project: Satellite-assisted localization and communication systems for emergency services," *IEEE Aerospace and Electronic Systems Magazine*, vol. 28, no. 9, pp. 4–15, 2013.

[14] A. Boukerche, B. Turgut, N. Aydin, M. Z. Ahmad, L. Boloni, and D. Turgut, "Routing protocols in ad hoc networks: A survey," *Computer Networks*, vol. 55, no. 13, pp. 3032 – 3080, 2011.

[15] Y. Jahir, M. Atiquzzaman, H. Refai, A. Paranjothi, and P. G. LoPresti, "Routing protocols and architecture for disaster area network: A survey," *Ad Hoc Networks*, vol. 82, pp. 1 – 14, 2019.

[16] E. K. Markakis, I. Politis, A. Lykourgiotis, Y. Rebahi, G. Mastorakis, C. X. Mavromoustakis, and E. Pallis, "Efficient next generation emergency communications over multi-access edge computing," *IEEE Communications Magazine*, vol. 55, no. 11, pp. 92–97, 2017.

[17] M. Usman, A. A. Gebremariam, U. Raza, and F. Granelli, "A software-defined device-to-device communication architecture for public safety applications in 5g networks," *IEEE Access*, vol. 3, pp. 1649–1654, 2015.

[18] M. N. Tehrani, M. Uysal, and H. Yanikomeroglu, "Device-to-device communication in 5g cellular networks: challenges, solutions, and future directions," *IEEE Communications Magazine*, vol. 52, no. 5, pp. 86–92, May 2014.

[19] G. Fodor, S. Roger, N. Rajatheva, S. B. Slimane, T. Svensson, P. Popovski, J. M. B. D. Silva, and S. Ali, "An overview of device-to-device communications technology components in METIS," *IEEE Access*, vol. 4, pp. 3288–3299, 2016.

[20] H. Nishiyama, M. Ito, and N. Kato, "Relay-by-smartphone: realizing multihop device-to-device communications," *IEEE Communications Magazine*, vol. 52, no. 4, pp. 56–65, 2014.

[21] H. Ahmad, M. Agiwal, N. Saxena, and A. Roy, "D2D-based survival on sharing for critical communications," *Wireless Networks*, vol. 24, no. 6, pp. 2283–2295, 2018.

[22] A. S. Muriel Medard, *Network Coding: Fundamentals and Applications*. Academic Press, 2011.

[23] B. Shrader and N. Jones, "Systematic wireless network coding," in *Military Communications Conference, 2009. MILCOM 2009. IEEE*, 2009, pp. 1–7.

[24] P. Pakzad, C. Fragouli, and A. Shokrollahi, "Coding schemes for line networks," in *Proceedings. International Symposium on Information Theory (ISIT)*, Sept 2005, pp. 1853–1857.

[25] D.-D. Tan and M. A. Vazquez-Castro, "Efficient communication over cellular networks with network coding in emergency scenarios," in *2015 2nd International Conference on Information and Communication Technologies for Disaster Management (ICT-DM)*, 2015, pp. 71–78.

[26] A. Kumbhar, F. Koohifar, I. Guvenc, and B. Mueller, "A survey on legacy and emerging technologies for public safety communications," *IEEE Communications Surveys Tutorials*, vol. 19, no. 1, pp. 97–124, 2017.

[27] N. D. Han, Y. Chung, and M. Jo, "Green data centers for cloud-assisted mobile ad hoc networks in 5g," *IEEE Network*, vol. 29, no. 2, pp. 70–76, 2015.

[28] J. Li, X. Li, Y. Gao, Y. Gao, and R. Zhang, "Dynamic cloudlet-assisted energy-saving routing mechanism for mobile ad hoc networks," *IEEE Access*, vol. 5, pp. 20 908–20 920, 2017.

[29] P. Ostovari, J. Wu, and A. Khreishah, *Network Coding Techniques for Wireless and Sensor Networks*. Spinger, 2013.

[30] J. Joy, Y.-T. Yu, M. Gerla, S. Wood, J. Mathewson, and M.-O. Stehr, "Network coding for content-based intermittently connected emergency networks," in *Proceedings of the 19th Annual International Conference on Mobile Computing & Networking*, ser. MobiCom '13, 2013, pp. 123–126.

[31] A. Altamimi and T. Gulliver, "On network coding in intermittently connected networks," in *IEEE 80th Vehicular Technology Conference (VTC Fall)*, Sept 2014, pp. 1–5.

[32] H. V. Nguyen, Z. Babar, S. X. Ng, M. Mazzotti, L. Iacobelli, and L. Hanzo, "Network coded mimo aided cooperative communications in the ambulance-and-emergency area," *Procedia Computer Science*, vol. 40, pp. 214 – 221, 2014.

[33] M. A. Pimentel-Nino, M. A. Vazquez-Castro, and I. Hernaez-Corres, "Perceptual semantics for video in situation awareness," in *The Ninth International Conference on Systems and Networks Communications*, Oct 2014, pp. 2403–2407.

[34] E. Magli, M. Wang, P. Frossard, and A. Markopoulou, "Network coding meets multimedia: A review," *IEEE Transactions on Multimedia*, vol. 15, no. 5, pp. 1195–1212, 2013.

[35] H. Seferoglu and A. Markopoulou, "Video-aware opportunistic network coding over wireless networks," *IEEE Journal on Selected Areas in Communications*, vol. 27, no. 5, pp. 713–728, 2009.

[36] C. Zhan and K. Gao, "Video delivery in heterogeneous wireless networks with network coding," *IEEE Wireless Communications Letters*, vol. 5, no. 5, pp. 472–475, 2016.

[37] P. Ostovari, J. Wu, A. Khreishah, and N. B. Shroff, "Scalable video streaming with helper nodes using random linear network coding," *IEEE/ACM Transactions on Networking*, vol. 24, no. 3, pp. 1574–1587, 2016.

[38] M. Esmaeilzadeh, P. Sadeghi, and N. Aboutorab, "Random linear network coding for wireless layered video broadcast: General design methods for adaptive feedback-free transmission," *IEEE Transactions on Communications*, vol. 65, no. 2, pp. 790–805, 2017.

[39] The European Telecommunications Standards Institute, "Network functions virtualisation (NFV); use cases," in *GS NFV 001 (V1.1.1)*, Oct. 2013.

[40] M. A. Vazquez-Castro and P. Saxena, "Network coding over satellite: From theory to design and performance," in *Volume 154 of the series Lecture Notes of the Institute for Computer Sciences, Social Informatics and Telecommunications Engineering*, Sept. 2015, pp. 315–327.

[41] J. Ordonez-Lucena, P. Ameigeiras, D. Lopez, J. J. Ramos-Munoz, J. Lorca, and J. Folgueira, "Network slicing for 5g with sdn/nfv: Concepts, architectures, and challenges," *IEEE Communications Magazine*, vol. 55, no. 5, pp. 80–87, 2017.

[42] V. Eramo, M. Ammar, and F. G. Lavacca, "Migration energy aware reconfigurations of virtual network function instances in nfv architectures," *IEEE Access*, vol. 5, pp. 4927–4938, 2017.

[43] J. Kang, O. Simeone, and J. Kang, "On the trade-off between computational load and reliability for network function virtualization," *IEEE Communications Letters*, vol. 21, no. 99, pp. 1767–1770, 2017.

[44] SDxCentral, "SDN controllers, cloud networking and more," 2017 Network Virtualization Report, Tech. Rep., 2017.

[45] Y. Li and M. Chen, "Software-defined network function virtualization: A survey," *IEEE Access*, vol. 3, pp. 2542–2553, 2015.

[46] The European Telecommunications Standards Institute, "Network functions virtualisation (nfv); management and orchestration," in *ETSI GS NFV-MAN 001 V1.1.1*, Dec. 2014.

[47] P. Saxena and M. A. Vazquez-Castro, "Link layer systematic random network coding for DVB-S2X/RCS," *Communications Letters, IEEE*, vol. 19, no. 7, pp. 1161–1164, 2015.

[48] S. Wunderlich, F. Gabriel, S. Pandi, F. H. P. Fitzek, and M. Reisslein, "Caterpillar RLNC (CRLNC): A practical finite sliding window rlnc approach," *IEEE Access*, vol. 5, no. 99, pp. 20 183–20 197, 2017.

[49] M. Hua, S. B. Damelin, J. Sun, and M. Yu, "The truncated & supplemented Pascal matrix and applications," *Involve Journal of Mathematics*, vol. 11, no. 2, pp. 243–251, 2018.

[50] L. Lu, M. Xiao, M. Skoglund, L. K. Rasmussen, G. Wu, and S. Li, "Efficient wireless broadcasting based on systematic binary deterministic rateless codes," in *2010 IEEE International Conference on Communications*, 2010, pp. 1–6.

[51] Y. Li, E. Soljanin, and P. Spasojevic, "Effects of the generation size and overlap on throughput and complexity in randomized linear network coding," *IEEE Transactions on Information Theory*, vol. 57, no. 2, pp. 1111–1123, 2011.

[52] A. Paramanathan, M. V. Pedersen, D. E. Lucani, F. H. P. Fitzek, and M. Katz, "Lean and mean: network coding for commercial devices," *IEEE Wireless Communications*, vol. 20, no. 5, pp. 54–61, 2013.

[53] M. A. Vazquez-Castro, P. Saxena, T. Do-Duy, T. Vamstad, and H. Skinnemoen, "SatNetCode: Functional design and experimental validation of network coding over satellite," in *the International Symposium on Networks, Computers and Communications (ISNCC)*, 2018.

[54] A. M. Zubkov and A. A. Serov, "A complete proof of universal inequalities for the distribution function of the binomial law," *Theory of Probability & Its Applications*, vol. 57, no. 3, pp. 539–544, 2013.

[55] A. C. Dalal, *Searching and sorting algorithms*. Supplementary Lecture Notes, CS117, 2004.

[56] C. Trenchea, *Lecture Notes on Numerical Mathematical Analysis, MATH1070*. University of Pittsburgh, 2014.

[57] Y. Chen, T. Farley, and N. Ye, "Qos requirements of network applications on the internet," *Inf. Knowl. Syst. Manag.*, vol. 4, no. 1, pp. 55–76, 2004.

[58] D. C. Salyers, A. D. Striegel, and C. Poellabauer, "Wireless reliability: Rethinking 802.11 packet loss," in *2008 International Symposium on a World of Wireless, Mobile and Multimedia Networks*, 2008, pp. 1–4.

[59] T. K. Dikaliotis, A. G. Dimakis, T. Ho, and M. Effros, "On the delay of network coding over line networks," in *2009 IEEE International Symposium on Information Theory*, 2009, pp. 1408–1412.

[60] M. Macit, V. C. Gungor, and G. Tuna, "Comparison of qos-aware single-path vs. multi-path routing protocols for image transmission in wireless multimedia sensor networks," *Ad Hoc Networks*, vol. 19, pp. 132 – 141, 2014.

[61] G. Angelopoulos, M. Médard, and A. P. Chandrakasan, *Energy-Aware Hardware Implementation of Network Coding*. Springer Berlin Heidelberg, 2011, pp. 137–144.

[62] R. A. Cacheda, D. C. García, A. Cuevas, F. J. G. Castaño, J. H. Sánchez, G. Koltsidas, V. Mancuso, J. I. M. Novella, S. Oh, and A. Pantò, *QoS Requirements For Multimedia Services*. Springer US, 2007, pp. 67–94.

[63] G. Garrammone, "On decoding complexity of reed-solomon codes on the packet erasure channel," *IEEE Communications Letters*, vol. 17, no. 4, pp. 773–776, 2013.

[64] V. Stankovic, R. Hamzaoui, and Z. Xiong, "Efficient channel code rate selection algorithms for forward error correction of packetized multimedia bitstreams in varying channels," *IEEE Transactions on Multimedia*, vol. 6, no. 2, pp. 240–248, 2004.

[65] J. Cloud, D. J. Leith, and M. Medard, "Network coded TCP (CTCP) performance over satellite networks," in *SPACOMM 2014: The Sixth International Conference on Advances in Satellite and Space Communications*, 2014, pp. 1–4.

[66] M. A. Awal, K. Kanchanasut, and Y. Tsuchimoto, "Multicast packet loss measurement and analysis over unidirectional satellite network," in *Technologies for Advanced Heterogeneous Networks*. Springer Berlin Heidelberg, 2005, pp. 254–268.

[67] Y. Shi, Y. E. Sagduyu, J. Zhang, and J. H. Li, "Adaptive coding optimization in wireless networks: Design and implementation aspects," *IEEE Transactions on Wireless Communications*, vol. 14, no. 10, pp. 5672–5680, 2015.

[68] J. D. Ellis and M. B. Pursley, "Adaptive transmission protocols for fountain-coded multicast in packet radio networks," *IEEE Transactions on Communications*, vol. 65, no. 4, pp. 1786–1796, April 2017.